REPORT No. 35.

APRIL, 1950.

THE COLLEGE OF AERONAUTICS

CRANFIELD

A Comparison of the Calculated Profile Drag Coefficients of Various Low-Drag Wing Sections.*

-by-

E. M. Dowlen. D.C.Ae.

Department of Aerodynamics.

--oOo--

SUMMARY

The profile drag-coefficients of a number of low-drag wings with straight trailing edges have been calculated.

A comparison is made with other low-drag and conventional sections which indicates an increase in profile drag, for a given transition point position, with rearward movement of the position of maximum velocity and with increase of trailing edge angle. Some experimental results obtained at low Reynolds number are included for comparison.

A shortened method of calculating the profile drag coefficient of an aerofoil is developed.

* Part of Thesis submitted for the College of Aeronautics Diploma, 1949.

YSB.

NOTATION.

c = Aerofoil chord.

t = Aerofoil thickness.

x = Distance along chord.

y = Distance normal to chord.

s = Distance along surface.

C_D = Drag coefficient.

C_{D_0} = Profile drag coefficient.

u = Local velocity inside boundary layer.

U = Local velocity outside boundary layer.

U_0 = Free steam velocity.

ρ = Density.

ν = Kinematic viscosity.

δ = Boundary layer thickness.

θ = Momentum thickness = $\int_0^{\delta} \frac{u}{U}(1 - \frac{u}{U})dy$.

R = Aerofoil Reynolds number = $U_0 c/\nu$.

R_δ = Boundary layer Reynolds number = $U_0 \delta/\nu$.

R_θ = Momentum thickness Reynolds number = $U_0 \theta/\nu$.

R_{θ_1} = Momentum thickness Reynolds number at transition.

n = Constant in equation for skin friction coefficient.

k = Constant in equation for skin friction coefficient.

b = $(1+n)k/R_c^{\,n}$.

p = Correction factor for integral I_2 = $(n-0{\cdot}2)/4$.

a = Factor = $(U/U_0)^{-0{\cdot}25}_{T.E.}$

I_1 = $\int_0^{T.P.} (U/U_0)^5 \, d(s/c)$.

I_2 = $\int_{T.P.}^{T.E.} (U/U_0)^4 \, d(s/c)$.

Suffix 'T.E.' refers to conditions at trailing edge.
Suffix 'T.P.' refers to conditions at transition point.

1. Introduction.

From the results of previous calculations (Ref. 1 -4) it appeared that for an aerofoil designed with maximum velocity far back from the leading edge, the drag (for a given transition point position, thickness chord ratio and Reynolds number) was greater than the corresponding drag for a so called conventional section. This increase offset in part the advantage gained from the greater extent of laminar boundary layer on such an aerofoil. It was also suspected that the shape of the trailing edge (concave, straight or convex) might have an influence on the profile drag (Ref. 10).

In this report the results of a number of calculations of the profile drag of various smooth wings in incompressible flow are presented. The majority of these sections had straight trailing edges.

Wind tunnel tests were made on four of these aerofoils (at a Reynolds number of about 1×10^6) in order to compare experimental and calculated results. These tests were not conclusive but demonstrate some of the difficulties to be met when trying to fix transition with wires at low Reynolds numbers.

2. Scope of Calculations.

The values of the profile drag of a number of symmetrical aerofoils at zero incidence were calculated by a method that is described in the Appendix. Some of the sections considered were of the N.A.C.A. 6A series of low drag wings with contours which are straight in the neighbourhood of the trailing edge (Ref. 5). Representative profiles are illustrated in Fig. 1 and pressure distributions are given in Fig. 3. The four sections indicated by the prefix ECA also had straight trailing edges. These last were tested in the wind tunnel to check the theoretical calculations. Their ordinates are given in Table I and Fig. 1, and their pressure distributions are given in Fig. 2. Thickness-chord ratios of 10, 15 and 20 percent have been covered by the calculations and in each case values of profile drag have been computed for Reynolds numbers of 10^6, 10^7 and 10^8 and transition points from 0·2 to 0·8 chords from the leading edge.

3. Results and Discussion of Calculations.

3.1. The results of the calculations are given in Table II and are presented graphically in Figures 4,5,6 as values of drag coefficient - vs - transition point position for each aerofoil at Reynolds numbers of 10^6, 10^7 and 10^8.

An alternative method of presentation as used in Ref. 11 is shown in Figures 7 - 11 where λ is the ratio of the profile drag coefficient of the wing to the profile drag coefficient of a flat plate with the same transition point position. The variation of λ with Reynolds number is small and a mean value of λ has been taken.

/3.2. Position of ...

3. 2. Position of Maximum Velocity.

It is convenient to use the position of maximum velocity on the aerofoil surface as a parameter rather than the position of maximum thickness. Most of the sections used were designed to have peak suctions at some fixed position. It is immediately obvious from the results that, for a given transition point position, thickness-chord ratio, and Reynolds number, rearward movement of the maximum velocity position has the effect of increasing the profile drag of aerofoils for which the shape of the velocity distribution aft of the peak suction is similar (see Figs. 4-6, 12). This effect tends to decrease with forward movement of the transition point position. Figure 12 illustrates the variation of profile drag with transition and peak suction position for 15 percent thick aerofoils at $R = 10^7$. A line is drawn on the figure to indicate the variation in drag coefficient of sections with transition at the peak suction position. It is evident that moving the transition point aft by designing the section with a far back peak suction gives a smaller reduction in drag than that obtained with a corresponding transition shift on a conventional type of section.

3. 3. Effect of Trailing Edge Shape.

The influence of the shape of the trailing edge on the profile drag of the section is illustrated in Fig. 13 where a comparison is made between N.A.C.A. 64A - 012 /straight trailing edges) and N.A.C.A. 64 - 012 (cusped trailing edge). It appears that the profile drag is reduced a little by reduction of trailing edge angle. The effect is more marked for far aft transition point positions (see Ref. 5 for a comparison of the velocity distributions on these two aerofoils). This effect can be associated with the fact that as the trailing edge angle is increased and the velocity distribution curve becomes more rounded, the value of the integral I_2 (the predominant factor in the expression for C_{D_0} (see the Appendix)) increases and hence so does the profile drag coefficient.

3. 4. Equivalent Transition Point Position.

A convenient way of comparing the effect of changes in aerofoil shape on the profile drag is by consideration of the 'equivalent transition point position'. This is defined (Ref. 10) as the mean transition point position required to give the same profile drag coefficient as that of a conventional section with a specified mean transition point position, other things (thickness-chord ratio and Reynolds number) being equal. In effect, for the same drag coefficient the transition point on a low drag wing lies behind the transition point on a conventional section. This rearward shift is plotted in Fig. 14 for a number of wings, including those of Refs. 2 -4.)

Two main effects are apparent:-

a. The rearward shift of the equivalent transition

/point is ...

point is least for transition point positions near the leading edge.

b. The maximum value of this rearward shift is in the main a function of position of peak suction, although some effect of trailing edge shape is apparent (cf. N.A.C.A. 64 - 012 and N.A.C.A. 64A - 012).

4. Scope of Experiments.

Drag measurements were made, using a wake survey method, for the four ECA sections. The models were of wooden construction of 15 inches chord, 30 inches between end plates in a spanwise direction, and were tested in No.1A tunnel at Cranfield.* Transition was observed by the china clay technique. Spanwise wires 0·01 inches in diameter were used to cause transition in the boundary layer. The wires were fixed to the wing surface by cellotape.

The results, corrected for wire drag are shown in Figs. 15 - 18. Fig. 19 shows drag as a function of 'Wire Transition Point' i.e. on the assumption that transition occurs at the wire. It would appear from the delay in the drag rise as the wire is moved forwards that transition at the low Reynolds number of the tests ($1{\cdot}1 \times 10^6$) is taking place over an appreciable region behind the wire and is not immediately provoked by the wire.

Tests were also made with a grid of fine string placed upstream of the model to produce a turbulent stream so as to move the transition point forward without the use of the wires fixed to the surface (see Figs. 15 - 18). Transition was again found to be indistinct and took place over a large region (this was checked by the readings of a surface pitot).

5. Discussion of the Experimental Results.

As already remarked at the low Reynolds number of the tests transition from laminar to turbulent flow takes place over quite an extensive region. The transition points given by the china clay and wire techniques lie at different points in this region, the difference appearing to be a function both of the local pressure gradient and also of the boundary layer thickness. In general the wire transition point, defined as the wire position for which the drag just begins to increase with further forward movement of the wire, lies some 12 - 22 percent chord ahead of the transition indicated by the china clay. Jones and Brown (Ref.6) find that the wire transition point lies some 13 - 17 percent ahead of the calculated transition point. The degree of tunnel turbulence is probably an important factor.

* The critical Reynolds number of a 6 inch sphere in this tunnel is about 3×10^5.

/An examination ...

An examination of Fig.19 shows that the shape of the curve of drag coefficient variation with wire position as measured is similar to the calculated curve of drag coefficient variation with transition point position and lies roughly parallel to it. The same broad conclusions about the effect of design maximum suction position apply.

Some flight tests made at the R.A.E. (Ref.3), where tape was used to fix transition, exhibit curves of very much the same shape as those found in the present tests, the tape transition point lying some 10 to 15 percent of the chord ahead of the calculated transition point. No such differences were observed in the tests of Ref.6 at high Reynolds number, and it would seem that further experimental work is required on the effect of spanwise turbulence wires on transition.

CONCLUSIONS.

1. The calculated profile drag coefficients of the series of low drag wings here considered are greater in all cases (for the same transition point position, thickness chord ratio and Reynolds number) than the corresponding profile drag coefficients of conventional sections (Fig.14).

2. This increase is a function in the main of the position of maximum velocity of the particular section - far back positions giving higher drag coefficients - and is most marked for positions of maximum velocity aft of about 45 percent chord (Fig.12).

3. This brings into question the desirability of designing wing sections with peak suctions further aft than about 0.45, in view of the practical difficulties of ensuring and maintaining the surface finish and freedom from waviness required for such extensive regions of laminar flow. We must also note the adverse effects on control characteristics and $C_{L\ max.}$ associated with the far back positions of maximum thickness required.

4. Changes in the shape of the trailing edge also produces changes in the profile drag coefficient. Profile drag is lowest for a cusped trailing edge and increases as the trailing edge becomes more convex. The increase is most apparent for far aft positions of transition (Fig.13).

5. The effect of thickness chord ratio on the profile drag is reduced for far back transition point positions, especially at high Reynolds numbers (Figs.7-11).

/6. Experimental ...

6. Experimental results at low Reynolds number indicate a large region of transition, but confirm qualitatively the predicted increase of drag coefficient with far back peak suction positions and confirm the reduction of this effect as the transition point moves forward (Fig. 19).

7. Further experimental work is required to check the calculated results, especially at high Reynolds numbers and in flight. Preliminary experiments to investigate in detail the effect of spanwise wires are desirable.

8. The calculation of aerofoil profile drag may be considerably shortened with no significant loss in accuracy. The profile drag coefficient may be expressed as a function of two integrals of the velocity distribution (see the Appendix).

REFERENCES

1.	H.B. Squire A.D. Young	The Calculation of the Profile Drag of Aerofoils. R and M 1838 (1937).
2.	N.E. Winterbottom H.B. Squire	Note on Further Wing Profile Drag Calculations. R.A.E. Rep. BA. 1634. (1940).
3.	R.C. Lock	Note on Profile Drag Calculations for Low-Drag Wings with Cusped Trailing Edges. R.A.E. Aero 2130 (1946) and Corrigenda (1948).
4.	A. Fage W.S. Walker	Experiments on Laminar-flow Aerofoil EQH 1260 in the William Froude National Tank and the 9 x 7 ft. Wind Tunnels at the National Physical Laboratory. R and M 2165 (1942).
5.	L.K. Loftin, Jnr.	Theoretical and Experimental Data for a Number of N.A.C.A. 6A Series Airfoil Sections. N.A.C.A. T.N. 1368 (1947).
6.	R. Jones A.F. Brown	Drag and Transition Experiments on Two Joukowski Aerofoils in the Compressed Air Tunnel. R and M 2110 (1941).
7.	G.E. Nitzberg	A Concise Theoretical Method for Profile Drag Calculations. N.A.C.A. ACR Feb. 1944. ARC 7707.
8.	Neal Tetervin	A Method for the Rapid Estimation of Turbulent Boundary Layer Thickness for Calculating Profile Drag. N.A.C.A. ACR L4G14 (1944).
9.	A.D. Young	Skin Friction in the Laminar Boundary Layer in Compressible Flow. College of Aeronautics Rep. No. 20 (1948).
10.	Sub-Committee of the Royal Aeronautical Society	Note on the Drag of Low Drag Wing Sections. Aerodynamics Data Sheets.
11.	Royal Aeronautical Society	Aerodynamics Data Sheets. Wings 02.04.02.

A P P E N D I X

Method of Calculation.

A1. The method used was essentially the same as that of Ref. 3, but was modified to reduce the labour involved.

In Ref. 8 the expression:-

$$(\theta/c)_{T.E.} = \frac{1}{(U/U_0)^{H+2}_{T.E.}} \left[\frac{(1+n)k}{R^n} \int_{T.P.}^{T.E.} (U/U_0)^{(H+1)(n+1)+1} d(s/c) + (\theta/c)^{n+1}_{T.P.} (U/U_0)^{(H+2)(n+1)}_{T.P.} \right]^{1/(n+1)} \quad \ldots\ldots (1)$$

is used to find the momentum thickness of the boundary layer at the trailing edge.

By combining this relation for the turbulent boundary layer with the equation[*]

$$(\theta/c)_{T.P.} = \frac{0{\cdot}664}{R^{\frac{1}{2}}(U/U_0)^3_{T.P.}} \left[\int_0^{T.P.} (U/U_0)^5 d(s/c) \right]^{\frac{1}{2}} \quad \ldots\ldots (2)$$

for the laminar boundary layer and with the expression

$$C_{D_0} = 2(\theta/c)_{T.E.} \left[(U/U_0)_{T.E.} \right]^{\frac{H+5}{2}} \quad \ldots\ldots (3)$$

we can derive an expression for the profile drag coefficient.

It was found that for a symmetrical aerofoil this relation could be replaced with no loss of accuracy by the expression

$$C_{D_0} = 4a \left[b(1+p)I_2 + (\theta/c)^{n+1}_{T.P.} (U/U_0)^{3{\cdot}5(n+1)}_{T.P.} \right]^{1/(n+1)}, \quad \ldots\ldots (4)$$

[*] This equation is a close approximation to one that can be derived from Ref. 9.

/where ...

where

$$a = (U/U_0)^{-0\cdot25}_{T.E.}, \qquad \ldots\ldots (5)$$

$$b = \frac{(1+n)k}{R^n} = \text{a function of } R_{\theta_1} \text{ and } R, \qquad \ldots\ldots (6)$$

$1+p$ = function of (R_{θ_1}) and is a correction factor, $\ldots\ldots (7)$

$$I_2 = \int_{T.P.}^{T.E.} (U/U_0)^4 \, d(s/c) \qquad \ldots\ldots (8)$$

and, as in (2)

$$(\theta/c)_{T.P.} = \frac{0\cdot664}{R^{\frac{1}{2}}(U/U_0)^3_{T.P.}} \left[I_1 \right]^{\frac{1}{2}},$$

where

$$I_1 = \int_0^{T.P.} (U/U_0)^5 \, d(s/c). \qquad \ldots\ldots (9)$$

The quantities $b(1+p)$, b, n and a are given in graphical form in Figs. 20 - 22 and the integrals I_1 and I_2 may be rapidly evaluated for any given pressure distribution.

A specimen calculation is shown in Table IV. Here the integrals I_1 and I_2 are evaluated with respect to x/c rather than s/c. It was found that this simplification resulted in an error in the calculated values of less than 1 percent for a 20 percent thick aerofoil (Table III).

A direct comparison with the method of Ref. 3 was obtained by calculating the drag coefficient for an N.A.C.A. 65,1-012 aerofoil at $R = 10^7$ with transition at 0·3c and 0·7c. The values obtained were 0·00652 and 0·00290 respectively. From Ref. 3 we obtain 0·00654 and 0·00286 (interpolated).

A Further Development.

A2. We can write equations (4) and (9) in the form

$$C_{D_0} = a\, F \left[I_1, I_2, (U/U_0)_{T.P.}, R \right]. \qquad \ldots\ldots (10)$$

Values of F are given in Table VII for various values of I_1, I_2 and $(U/U_0)_{T.P.}$ and $R = 10^7$, and are plotted in the form of a lattice in Fig. 23. Use of such a lattice and equation (10) enables the value of C_{D_0} for a given aerofoil to be obtained in a very short time, the calculation consisting mainly of the evaluation of the integrals I_1 and I_2. Comparison of results obtained using equation (10) with those of Ref. 2 shows equation (10) to give values of C_{D_0} some 2 to 4 percent too high (Table III). To cover a range of Reynolds numbers a series of such lattices would be required.

T A B L E I.

Ordinates of ECA Sections.

x/c	y/c	y/c
	ECA 1030	ECA 1050
0	0	0
.005	.0091	.0071
.010	.0128	.0099
.015	.0156	.0122
.025	.0200	.0156
.050	.0276	.0218
.075	.0331	.0263
.100	.0373	.0300
.150	.0433	.0357
.200	.0471	.0400
.250	.0491	.0433
.300	.0500	.0458
.350		.0477
.400	.0483	.0490
.450		.0498
.500	.0434	.0500
.550		.0496
.600	.0366	.0486
.700	.0280	.0438
.800	.0193	.0329
.900	.0102	.0175
.950	.0056	.0091
1.000	.0011	.0011

20 percent thick sections have all y/c multiplied by two.

ECA 1030A
As for 1030 until
.0500
.0484
.0441
.0380
.0305
.0219
.0121
.0068
.0011

TABLE II.

CALCULATED PROFILE DRAG COEFFICIENTS.

AEROFOIL SECTION	$R_c = 10^6$		$R_c = 10^7$		$R_c = 10^8$	
	T.P.	C_{D_0}	T.P.	C_{D_0}	T.P.	C_{D_0}
NACA 63A010			0·1	·00745	0·1	·00513
	0·3	·00956	0·3	·00603	0·3	·00403
	0·5	·00752	0·5	·00436	0·5	·00282
	0·7	·00559	0·7	·00285	0·7	·00170
NACA 64A010			0·1	·00742	0·1	·00517
	0·3	·00962	0·3	·00611	0·3	·00412
	0·5	·00765	0·5	·00442	0·5	·00290
	0·7	·00569	0·7	·00290	0·7	·00176
NACA 65A010			0·1	·00745	0·1	·00520
	0·3	·00980	0·3	·00615	0·3	·00419
	0·5	·00780	0·5	·00459	0·5	·00298
	0·7	·00571	0·7	·00294	0·7	·00178
NACA 63A015			0·1	·00816	0·1	·00578
	0·3	·01074	0·3	·00656	0·3	·00449
	0·5	·00813	0·5	·00457	0·5	·00296
	0·7	·00574	0·7	·00287	0·7	·00165
NACA 64A015			0·1	·00843	0·1	·00585
	0·3	·01082	0·3	·00681	0·3	·00459
	0·5	·00833	0·5	·00473	0·5	·00307
	0·7	·00594	0·7	·00294	0·7	·00174
NACA 65A015			0·1	·00853	0·1	·00591
	0·3	·01106	0·3	·00700	0·3	·00475
	0·5	·00859	0·5	·00497	0·5	·00322
	0·7	·00613	0·7	·00306	0·7	·00183
ECA 1030	0·2	·01040	0·1	·00732	0·1	·00521
	0·4	·00855	0·4	·00512	0·4	·00331
	0·6	·00652	0·6	·00354	0·6	·00223
	0·8	·00482	0·8	·00225	0·8	·00126
ECA 1050	0·2	·01092	0·1	·00741	0·1	·00534
	0·4	·00935	0·4	·00572	0·4	·00384
	0·6	·00733	0·6	·00414	0·6	·00264
	0·8	·00505	0·8	·00239	0·8	·00133

T A B L E II (Continued).

AEROFOIL SECTION	$R_c=10^6$		$R_c=10^7$		$R_c=10^8$	
	T.P.	C_{D_0}	T.P.	C_{D_0}	T.P.	C_{D_0}
ECA 2030	0·18	·01338	·08	·00973	·08	·00685
	0·27	·01208	·27	·00752	·27	·00505
	0·47	·00920	·47	·00521	·47	·00333
	0·67	·00671	·67	·00337	·67	·00196
ECA 2050	0·2	·01425	0·2	·00892	0·2	·00585
	0·4	·01204	0·4	·00731	0·4	·00490
	0·6	·00925	0·6	·00527	0·6	·00333
AN 514-011			0·2	·00719		
			0·4	·00557		
			0·6	·00373		
ECA 2030A	0·2	·01370	0·2	·00870	0·2	·00586
NACA 65,-012			0·3	·00652		
			0·7	·00290		
NACA 64,-012			0·1	·00774	0·1	·00535
	0·3	·01000	0·3	·00624	0·3	·00425
	0·5	·00771	0·5	·00440	0·5	·00285
	0·7	·00556	0·7	·00277	0·7	·00164

T A B L E III .

COMPARISON of RESULTS OBTAINED BY USE of FIG. 23.					
Method of Calculation	Trans. Point	C_D Top	C_D Bottom	C_{D_0}	
Winterbottom and Squire. (v. RAE.Rep BA1634).	0·4	·00816	·00576	·00696	20 percent thick wing of Ref. 2.
	0·6	·00554	·00404	·00479	
Fig. 23 using velocity distb^n along surface	0·4	·00846	·00585	·00715	
	0·6	·00573	·00406	·00490	
Fig. 23 using chordwise vel. distb^n.	0·4	·00839	·00584	·00711	
	0·6	·00564	·00406	·00485	

TABLE IV.

CALCULATION OF PROFILE DRAG FOR NACA 64$_2$-012.

AEROFOIL AT ZERO INCIDENCE

x/c	U/U_0	$U/U_0{}^4$	$U/U_0{}^5$	I_1	I_2
0	0	0	0	0	-
0·05	1·099	1·468	1·613	-	-
0·10	1·123	1·593	1·789	0·137	1·257
0·20	1·148	1·738	1·995	-	-
0·30	1·162	1·823	2·118	0·533	0·912
0·40	1·171	1·882	2·204	-	-
0·50	1·136	1·664	1·890	0·960	0·545
0·60	1·093	1·428	1·561	-	-
0·70	1·043	1·183	1·234	1·272	0·260
0·80	·989	·956	-	-	-
0·90	·935	·764	-	-	-
1·00	·881	·602	-	-	0

$a = 1·032$

For $R_c = 10^7$

1	Trans. Pt.	0·1	0·3	0·5	0·7	
2	$(U/U_0)_{T.P.}$	1·123	1·162	1·136	1·043	
3	$(U/U_0)^3_{T.P.}$	1·416	1·569	1·466	1·135	
4	$(\theta/c)_{T.P.} \times 10^5$	5·49	9·77	14·04	20·87	$= 0·664\sqrt{I_1}/R_c^{\frac{1}{2}}(U/U_0)^3_{T.P.}$
5	R_{θ_1}	617	1135	1595	2180	$= R_c(\theta/c)_{T.P.}(U/U_0)_{T.P.}$
6	n	0·214	0·201	0·195	0·190	From Fig. 21
7	$b(1 + p)$	·000382	·000419	·000438	·000452	From Fig. 20
8	$I_2 b(1 + p)$	·000480	·000382	·000239	·000117	$I_2 \times (7)$
9	$3·5(n + 1)$	4·25	4·20	4·18	4·165	From Table V
10	$(U/U_0)^{3·5(n+1)}_{T.P.}$	1·636	1·878	1·705	1·191	
11	$(\theta/c)^{n+1}_{T.P.} \times 10^6$	6·71	15·22	24·89	41·71	
12	(10) x (11)	·000011	·000029	·000042	·000050	
13	(8) + (12)	·000491	·000411	·000281	·000167	
14	$1/(n + 1)$	·824	·833	·837	·840	From Table VI
15	C_{D_0}	·00774	·00624	·00440	·00277	$(13)^{1/(n+1)} \times 4a$

TABLE V.

Values of $3 \cdot 5(n+1)$.

n	0	1	2	3	4	5	6	7	8	9
0·17	4·095	4·10	4·10	4·105	4·11	4·11	4·115	4·12	4·12	4·125
0·18	4·13	4·13	4·135	4·14	4·14	4·145	4·15	4·15	4·16	4·16
0·19	4·165	4·17	4·17	4·175	4·18	4·18	4·185	4·19	4·19	4·195
0·20	4·20	4·20	4·205	4·21	4·21	4·215	4·22	4·22	4·225	4·23
0·21	4·23	4·235	4·24	4·245	4·25	4·25	4·255	4·26	4·26	4·265
0·22	4·27	4·275	4·275	4·28	4·285	4·29	4·29	4·295	4·30	4·30
0·23	4·305	4·31	4·31	4·315	4·32	4·32	4·325	4·33	4·33	4·335
0·24	4·34	4·345	4·345	4·35	4·355	4·36	4·36	4·365	4·37	4·37

TABLE VI.

Values of $1/(n+1)$.

n	0	1	2	3	4	5	6	7	8	9
0·17	·855	·854	·853	·853	·852	·851	·850	·850	·849	·848
0·18	·847	·847	·846	·845	·844	·844	·843	·842	·842	·841
0·19	·840	·840	·839	·838	·837	·837	·836	·835	·835	·834
0·20	·833	·833	·832	·831	·831	·830	·829	·829	·828	·827
0·21	·827	·826	·825	·825	·824	·823	·822	·822	·821	·820
0·22	·820	·819	·818	·818	·817	·816	·816	·815	·814	·814
0·23	·813	·812	·812	·811	·810	·810	·809	·808	808	807
0·24	·807									

T A B L E VII.

RESULTS OF CALCULATION OF VALUES OF C_{D_0} FOR VARIOUS VALUES OF I_1, I_2, $(U/U_0)_{T.P.}$

$R = 10^7$

I_1	$(U/U_0)_{T.P.}$	$10^5 \times C_{D_0}/a$			
		I_2=1·5	I_2=1·1	I_2=0·7	I_2=0·3
0·100	1·00	864	674	468	241
0·097	1·20	854	667	465	241
0·095	1·40	838	654	458	240
0·50	1·00	897	698	493	264
0·48	1·20	891	698	491	267
0·47	1·40	888	697	494	270
0·90	1·00	908	711	504	276
0·87	1·20	910	713	508	282
0·85	1·40	908	715	513	288
1·30	1·00	917	722	516	290
1·26	1·20	924	729	522	298
1·23	1·40	926	732	527	304
1·70	1·00	932	732	526	303
1·65	1·20	935	740	532	310
1·61	1·40	936	743	539	316

Results are plotted in Fig. 23.

$$I_1 = \int_0^{T.P.} (U/U_0)^5 \, d(s/c).$$

$$I_2 = \int_{T.P.}^{T.E.} (U/U_0)^4 \, d(s/c).$$

BASIC SHAPES OF AEROFOIL SECTIONS

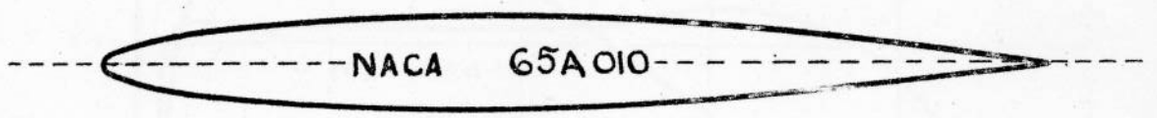

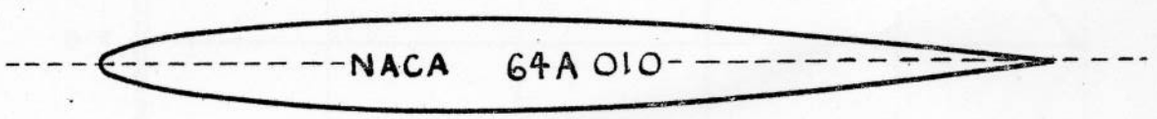

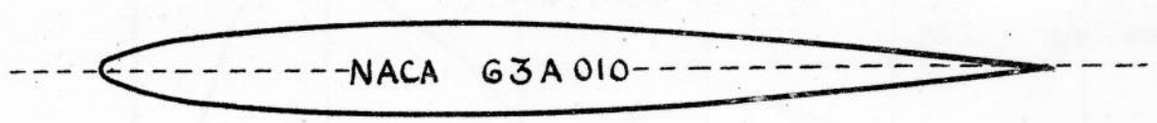

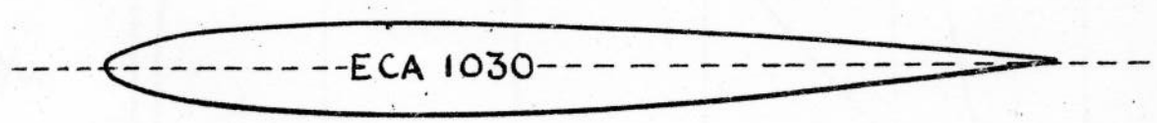

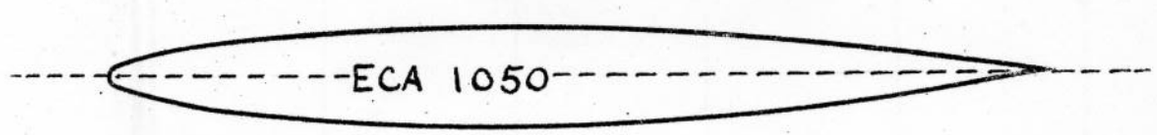

FIG 1

VELOCITY DISTRIBUTION FOR AEROFOILS USED IN WIND TUNNEL TESTS

(EXPERIMENTALLY DETERMINED)

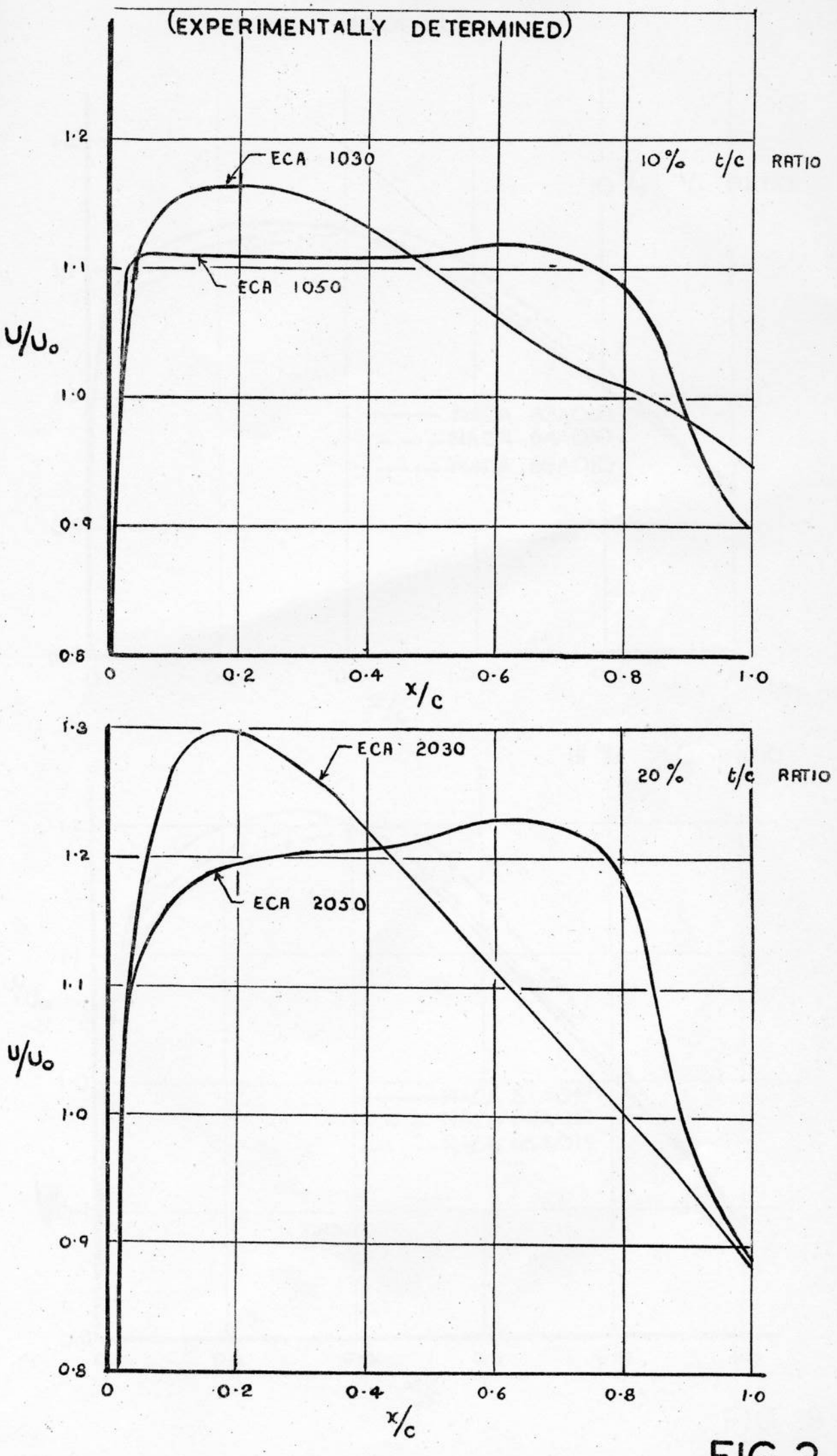

FIG 2

VELOCITY DISTRIBUTIONS FOR NACA 6A SERIES AEROFOILS

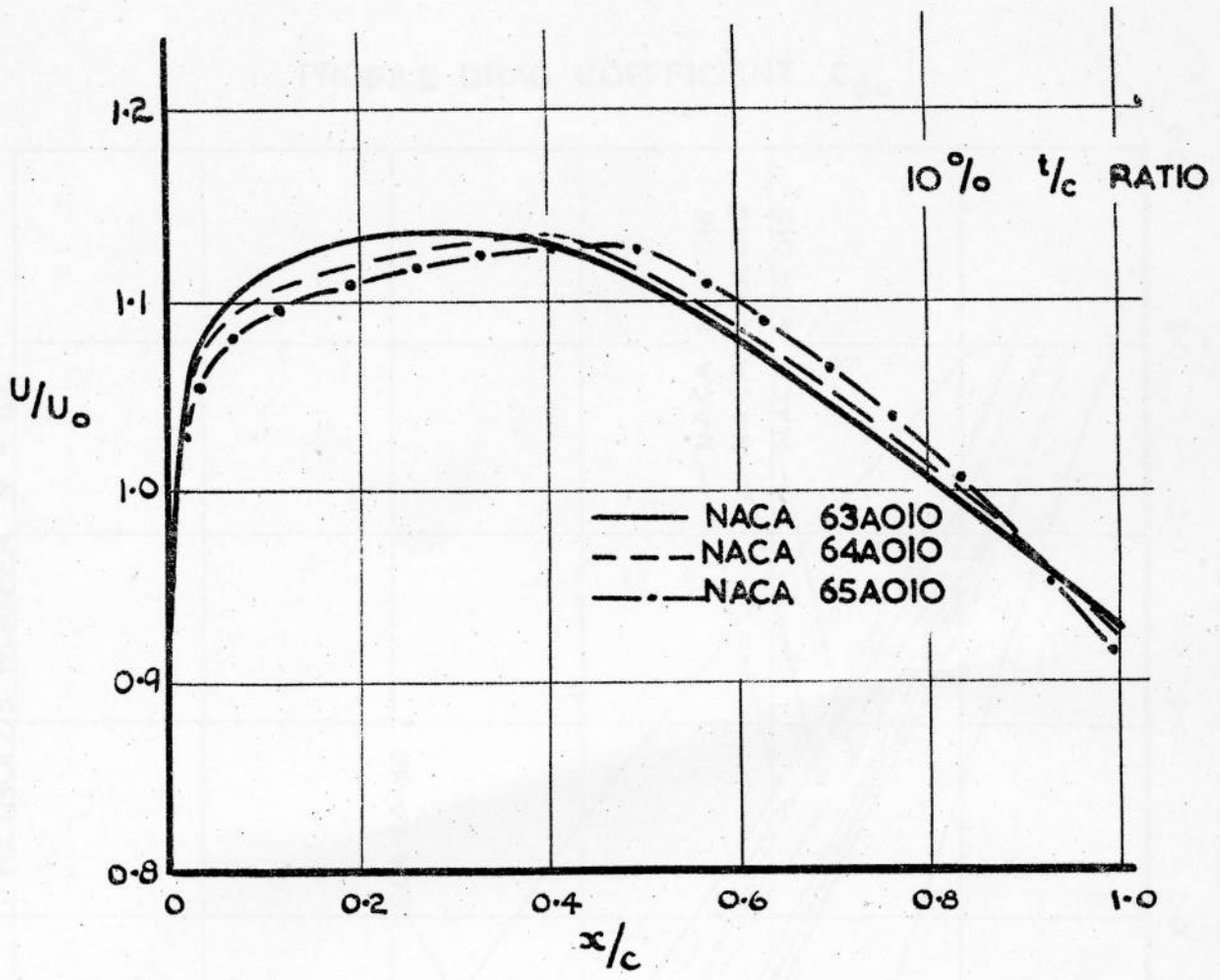

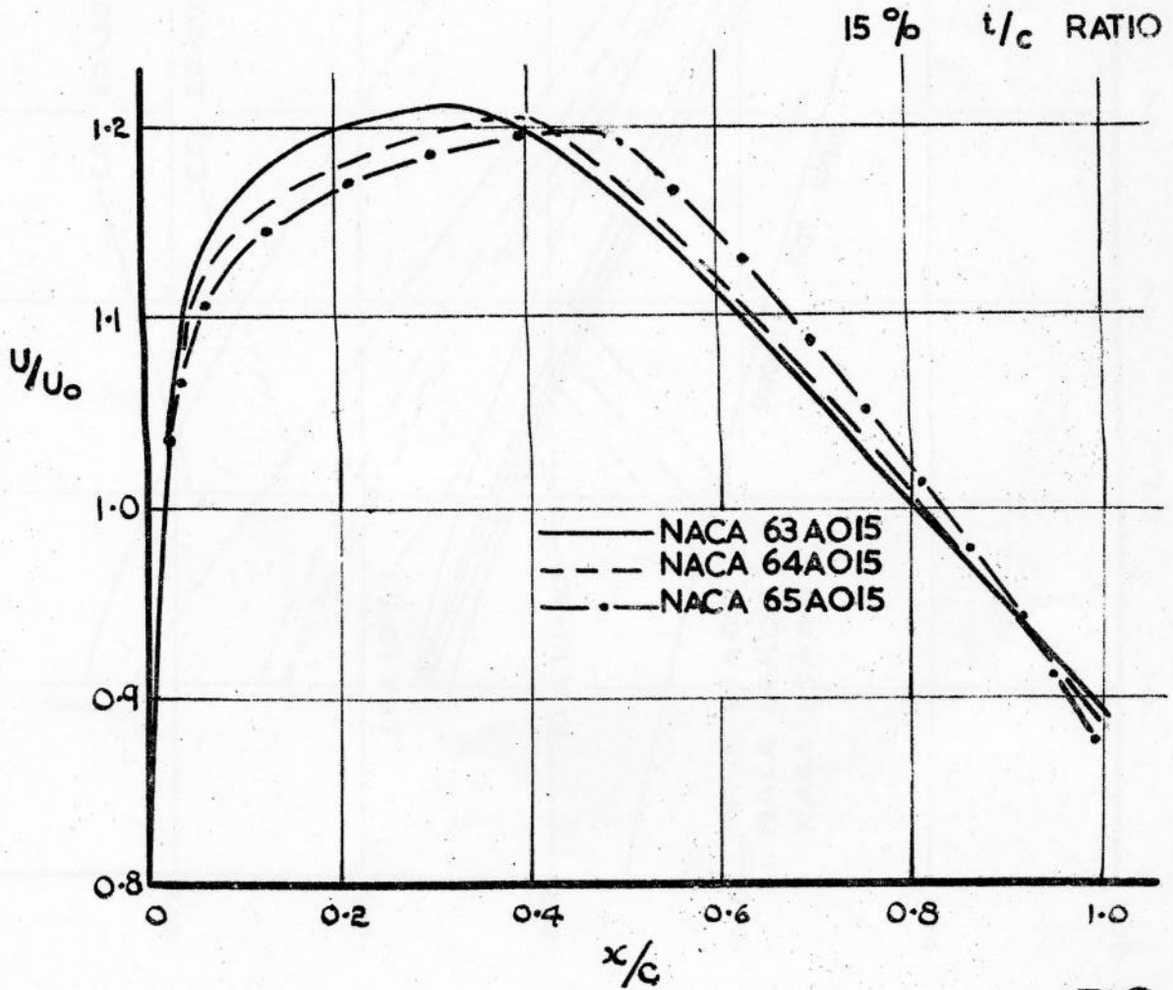

FIG 3

CALCULATED PROFILE DRAG OF NACA 6A SERIES AEROFOILS AND OF FOUR SPECIALLY DESIGNED SECTIONS

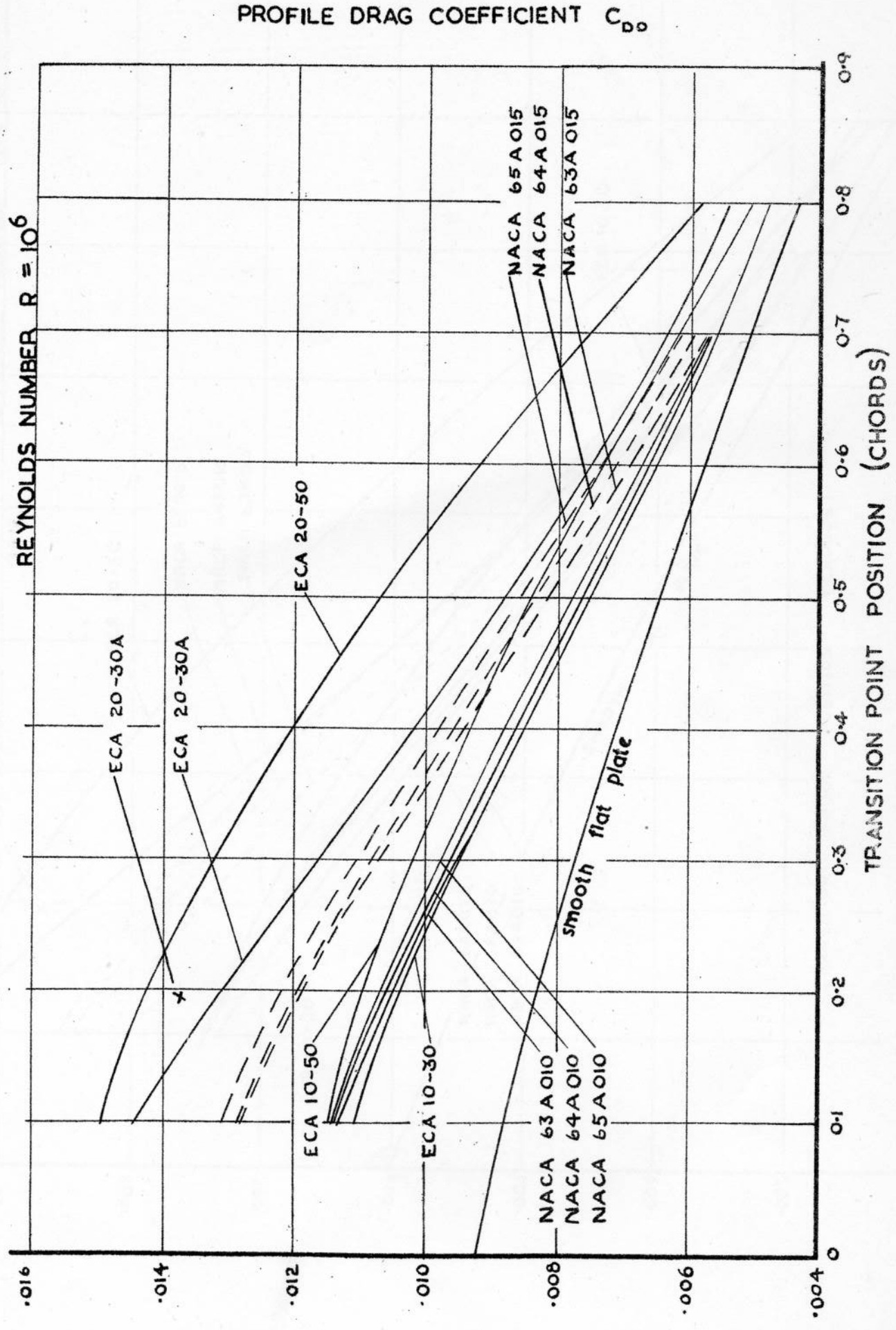

FIG 4

REPORT NO. 35

CALCULATED PROFILE DRAG OF NACA 6A SERIES AEROFOIL AND OF FOUR SPECIALLY DESIGNED SECTIONS

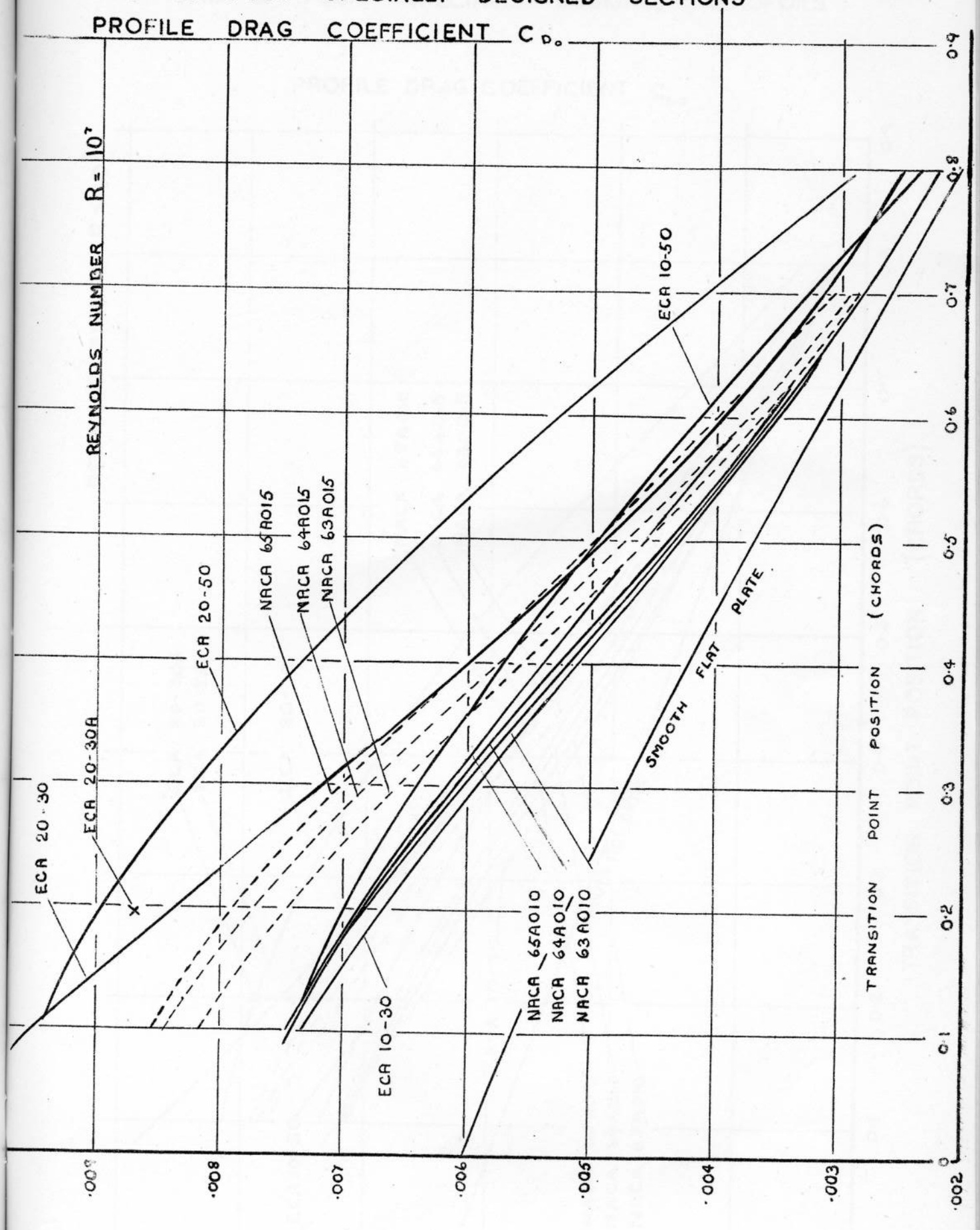

FIG 5

CALCULATED PROFILE DRAG OF NACA 6A SERIES AEROFOILS AND OF FOUR SPECIALLY DESIGNED AEROFOILS

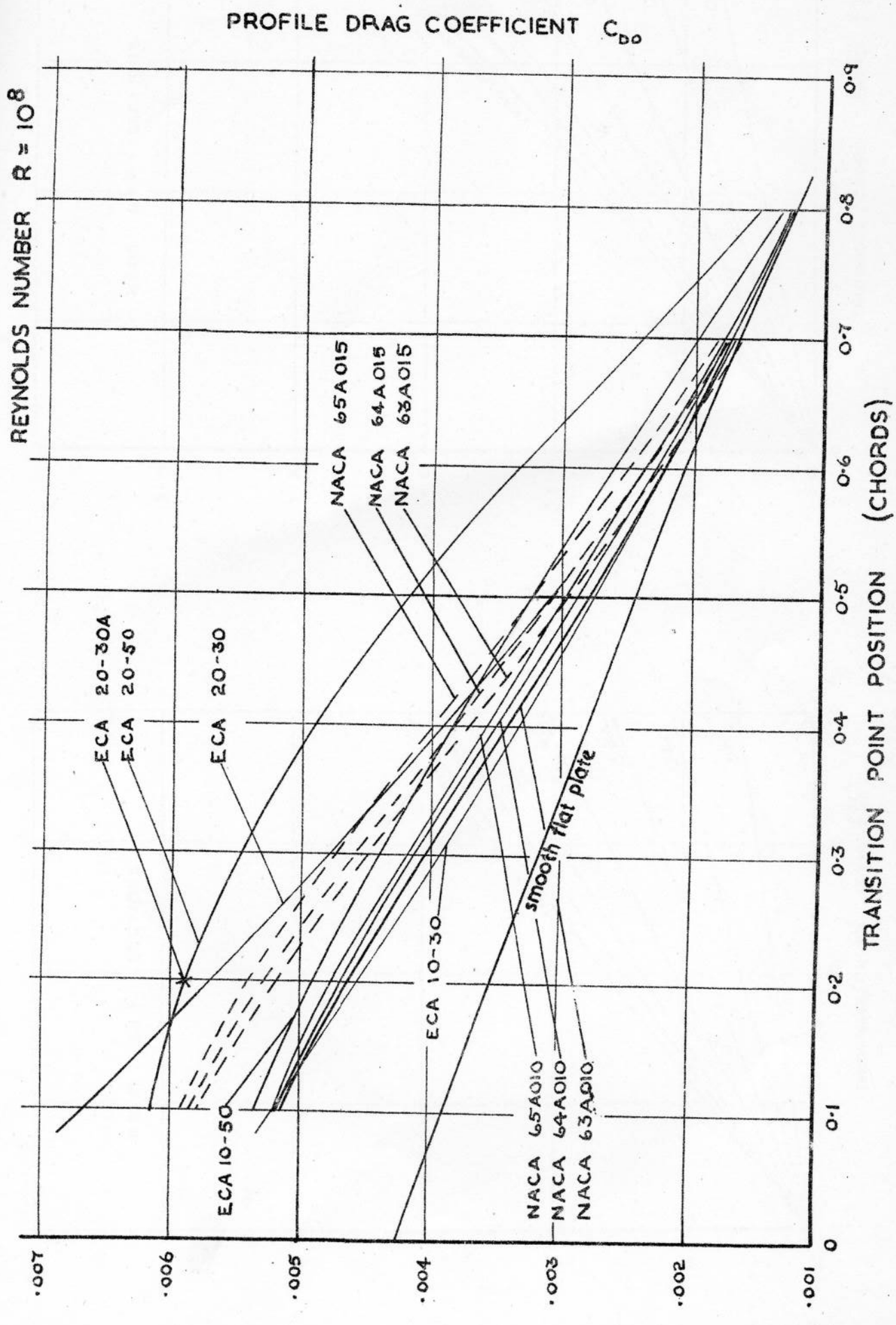

FIG 6

VALUES OF CORRECTION FACTOR λ

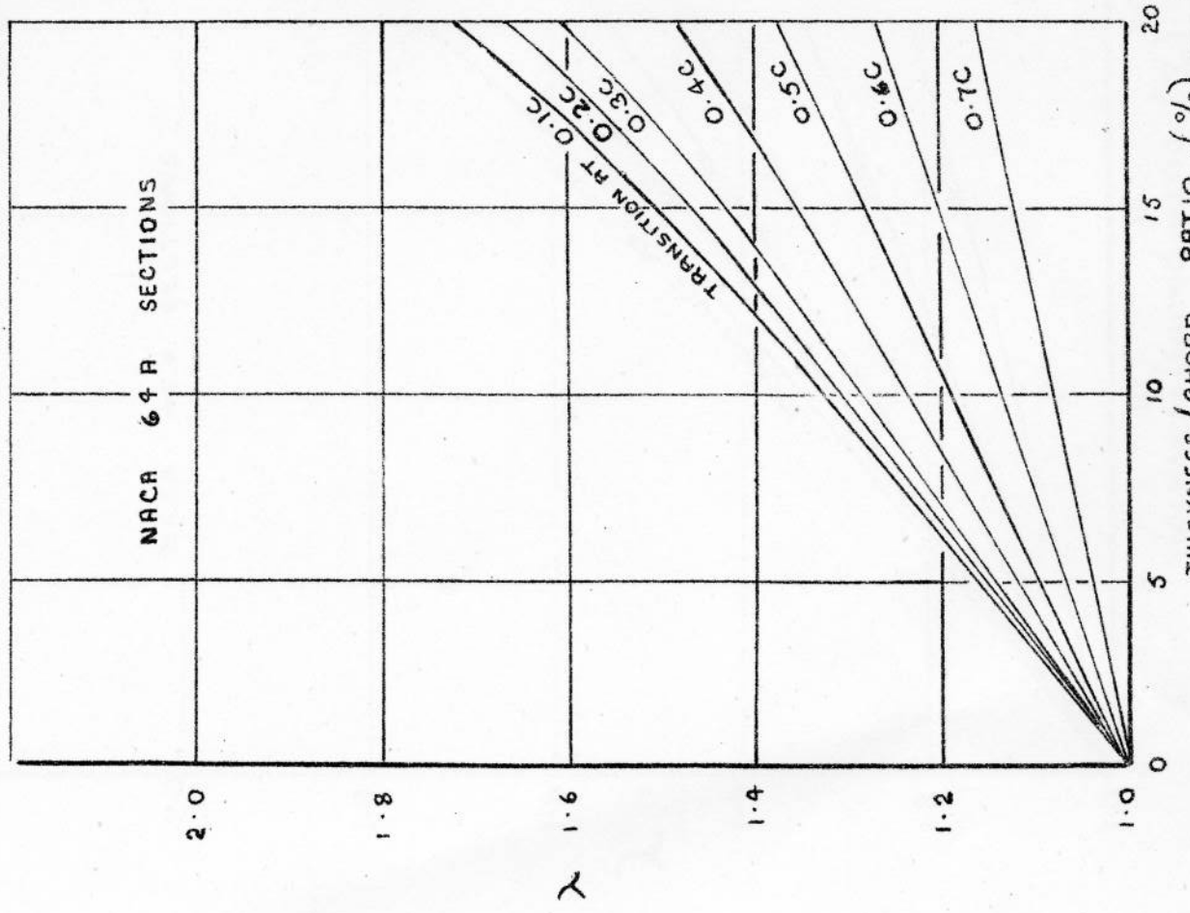

FIG 8

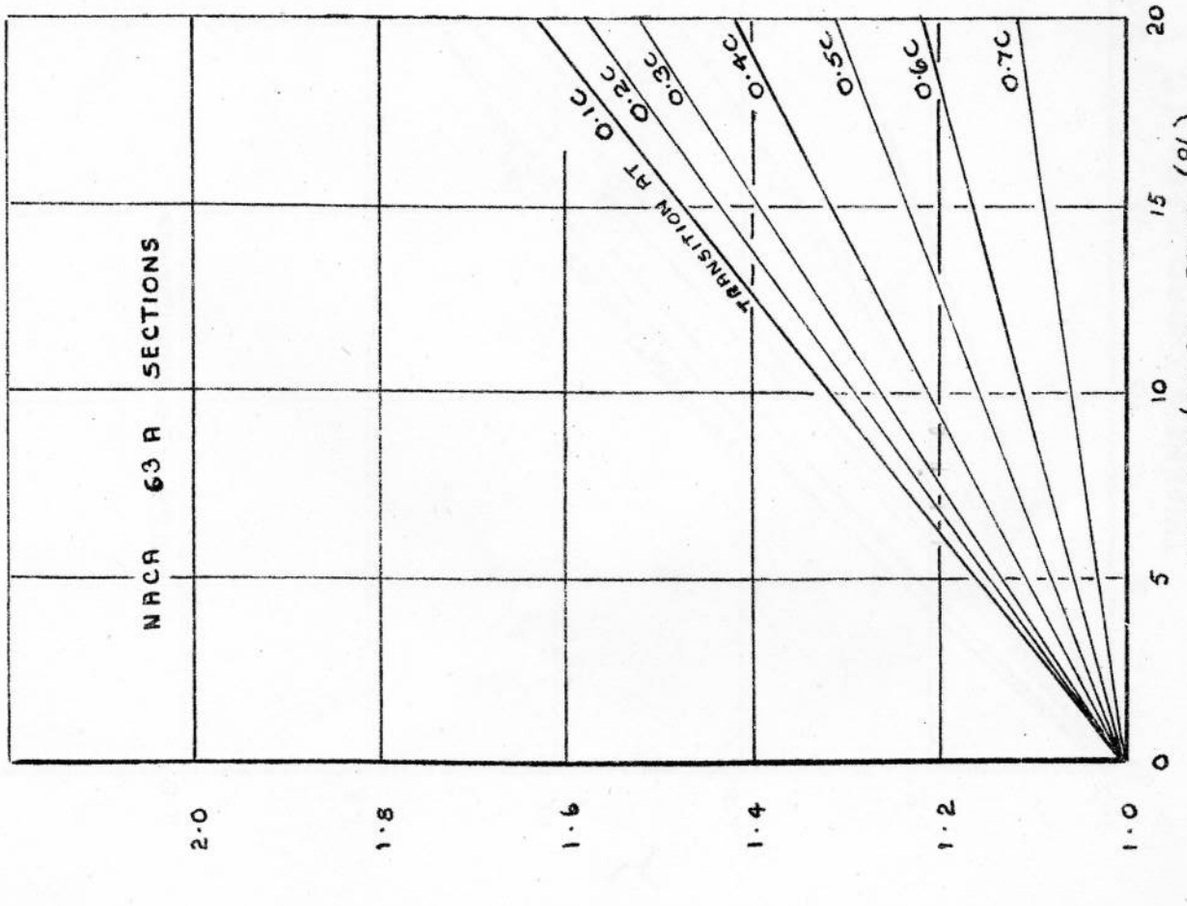

FIG 7

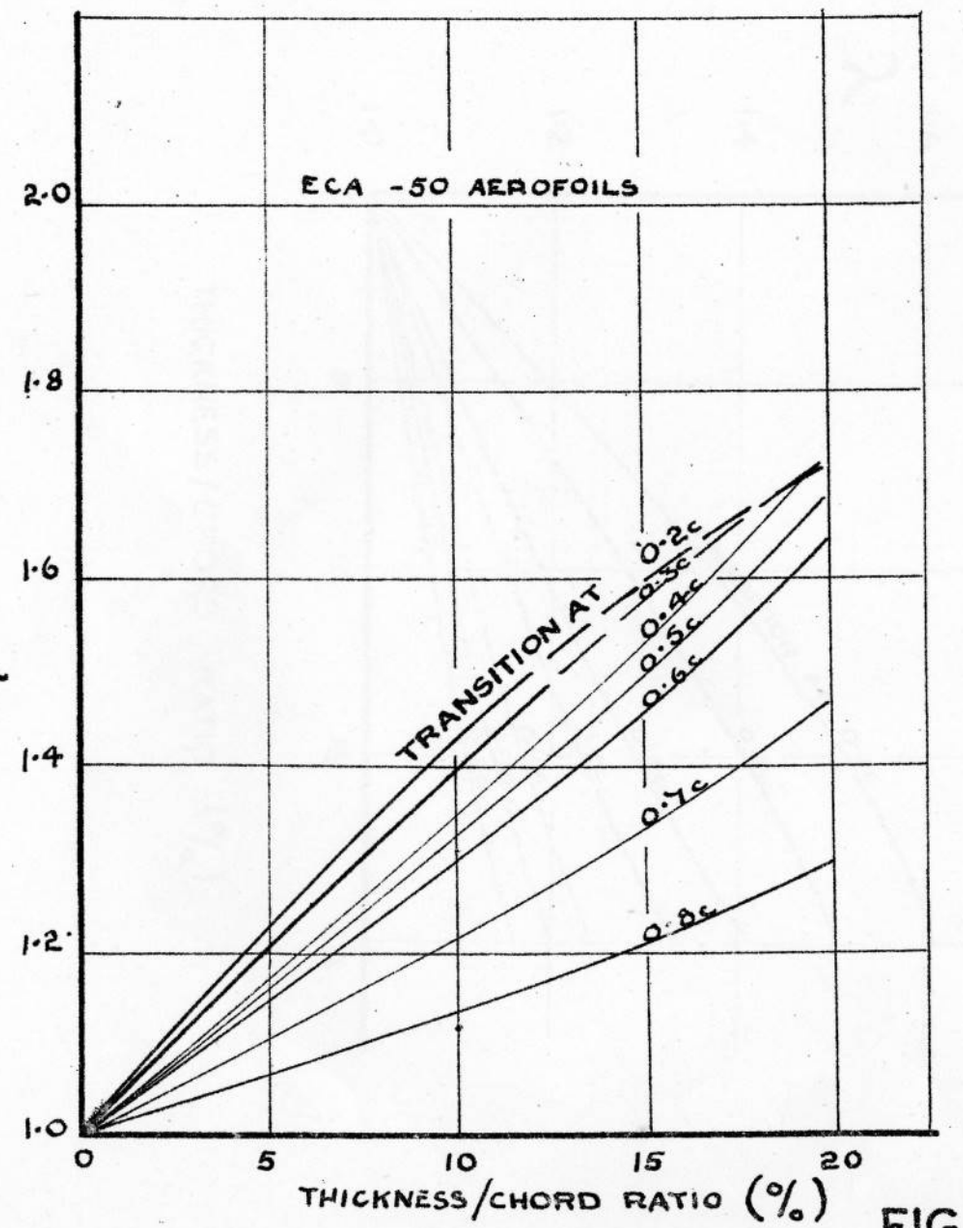
ECA -50 AEROFOILS
TRANSITION AT
0·2c
0·3c
0·4c
0·5c
0·6c
0·7c
0·8c
λ
2·0
1·8
1·6
1·4
1·2
1·0
0
5
10
15
20
THICKNESS/CHORD RATIO (%)

FIG 10

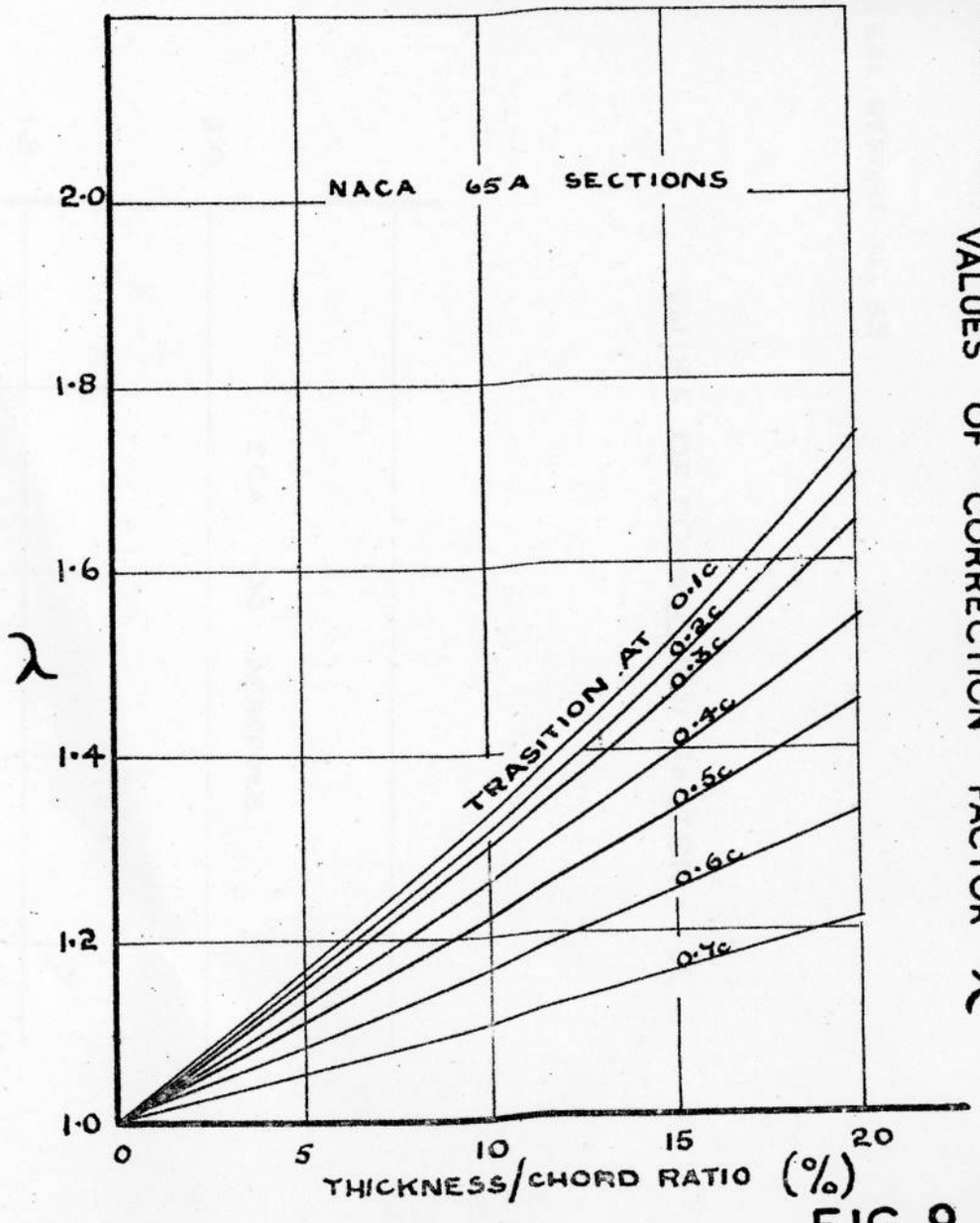
NACA 65A SECTIONS
TRASITION AT
0·1c
0·2c
0·3c
0·4c
0·5c
0·6c
0·7c
λ
2·0
1·8
1·6
1·4
1·2
1·0
0
5
10
15
20
THICKNESS/CHORD RATIO (%)

FIG 9

VALUES OF CORRECTION FACTOR λ

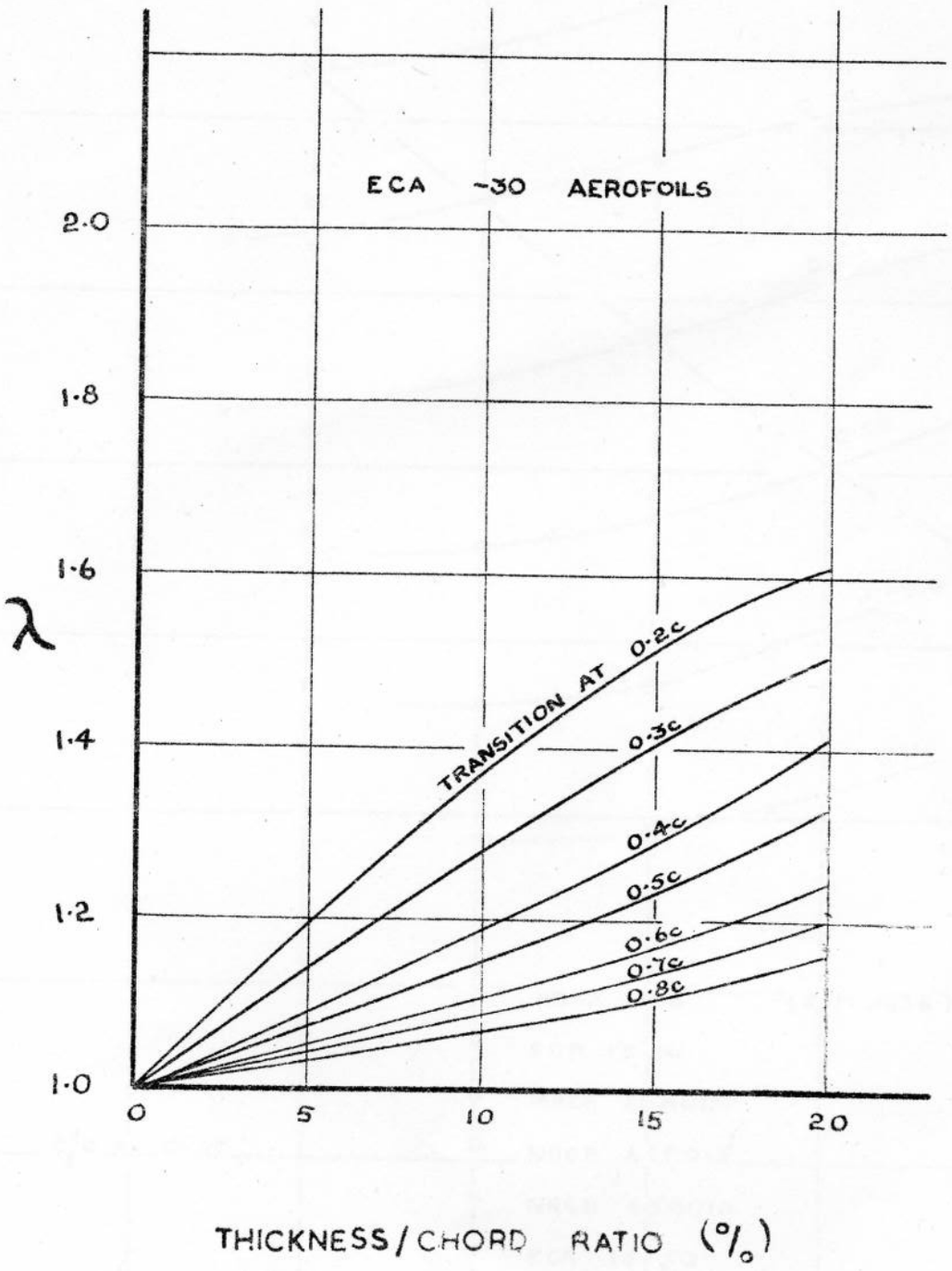

FIG 11

COLLEGE REPORT NO 35

EFFECT OF VARIATION OF POSITION OF MAXIMUM SUCTION ON THE PROFILE DRAG (VARIOUS AEROFOILS) STRAIGHT TRAILING EDGES

$R = 10^7$

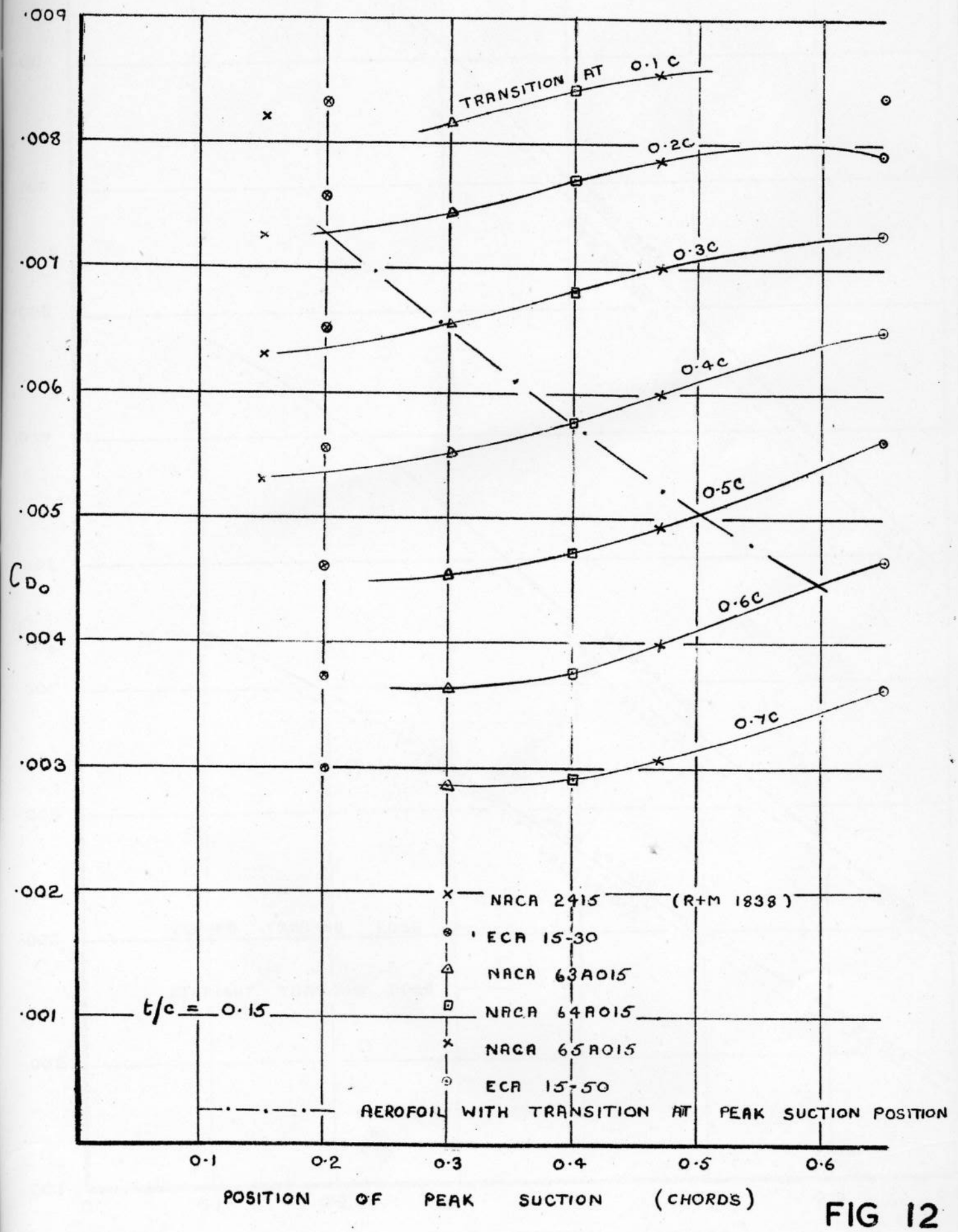

FIG 12

VARIATION OF PROFILE DRAG WITH CHANGE IN THE SHAPE OF THE TRAILING EDGE

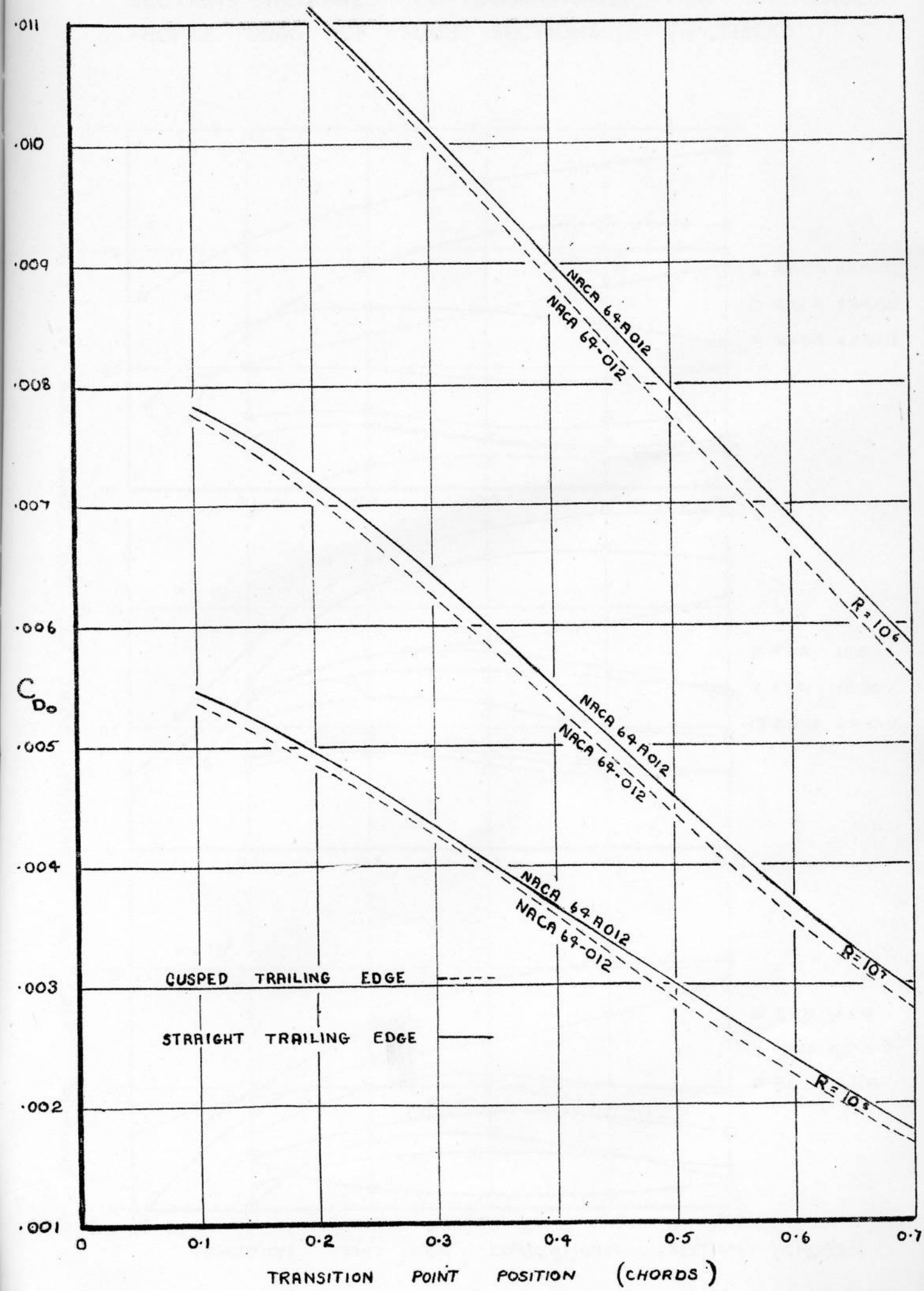

FIG 13

REARWARD SHIFT OF TRANSITION ON LOW-DRAG WING SECTIONS REQUIRED TO COMPENSATE FOR INCREASED PROFILE DRAG OF SUCH SECTIONS (12% THICK)

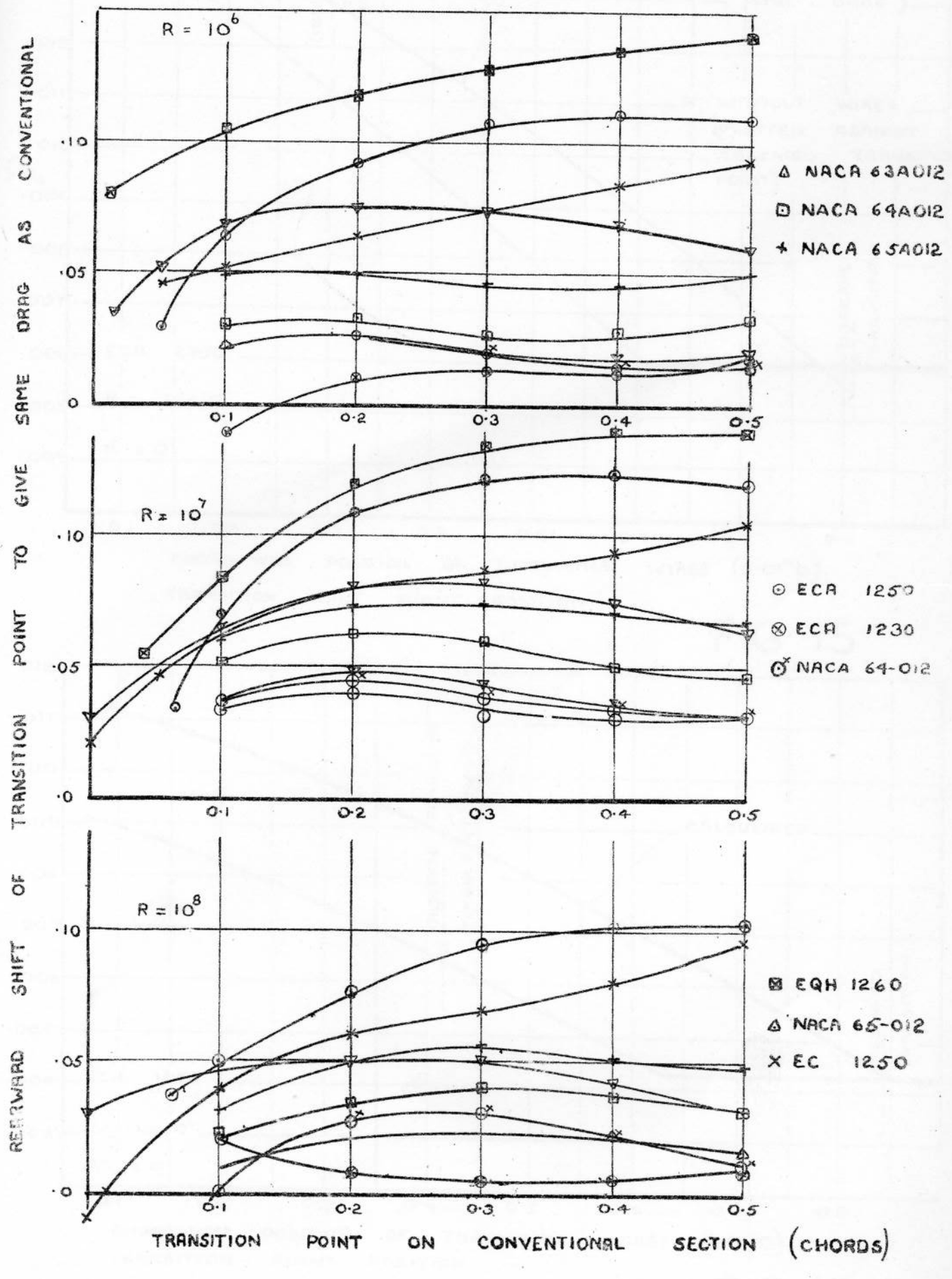

FIG 14

EXPERIMENTAL RESULTS FOR ECA 2030 AND ECA 1050 AEROFOILS

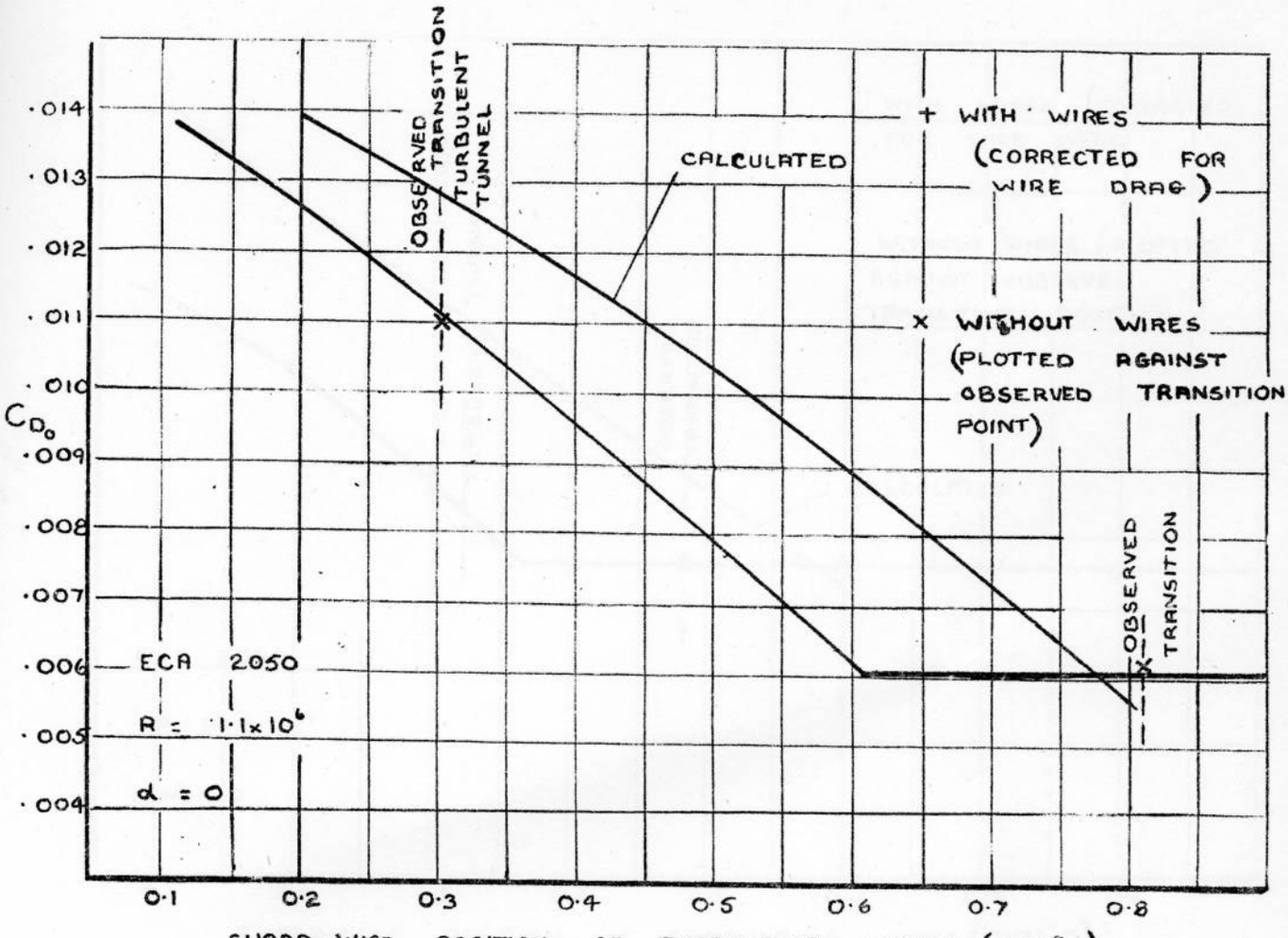

FIG 15

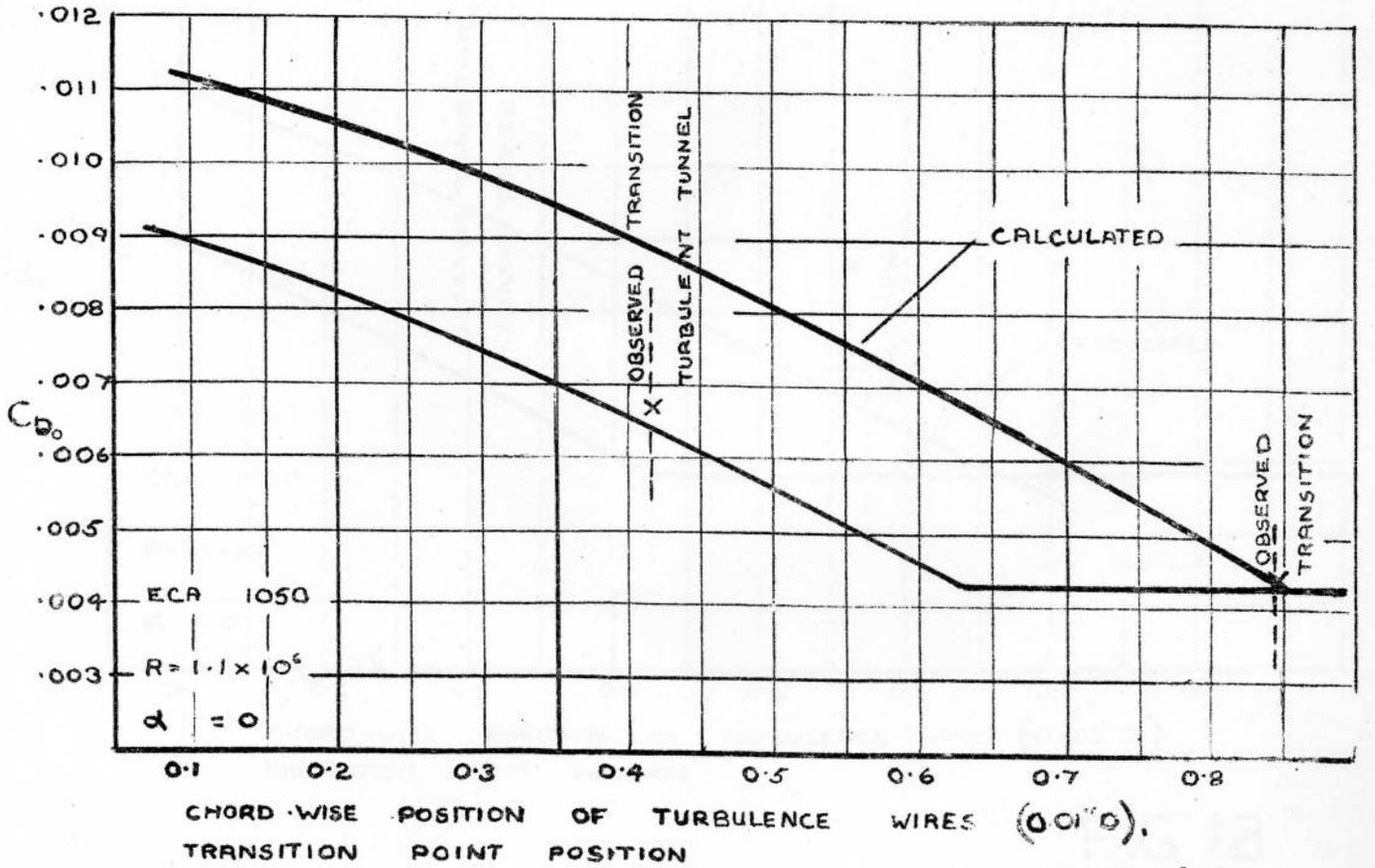

FIG 16

EXPERIMENTAL RESULTS FOR ECA 2030 AND ECA 1030 AEROFOILS

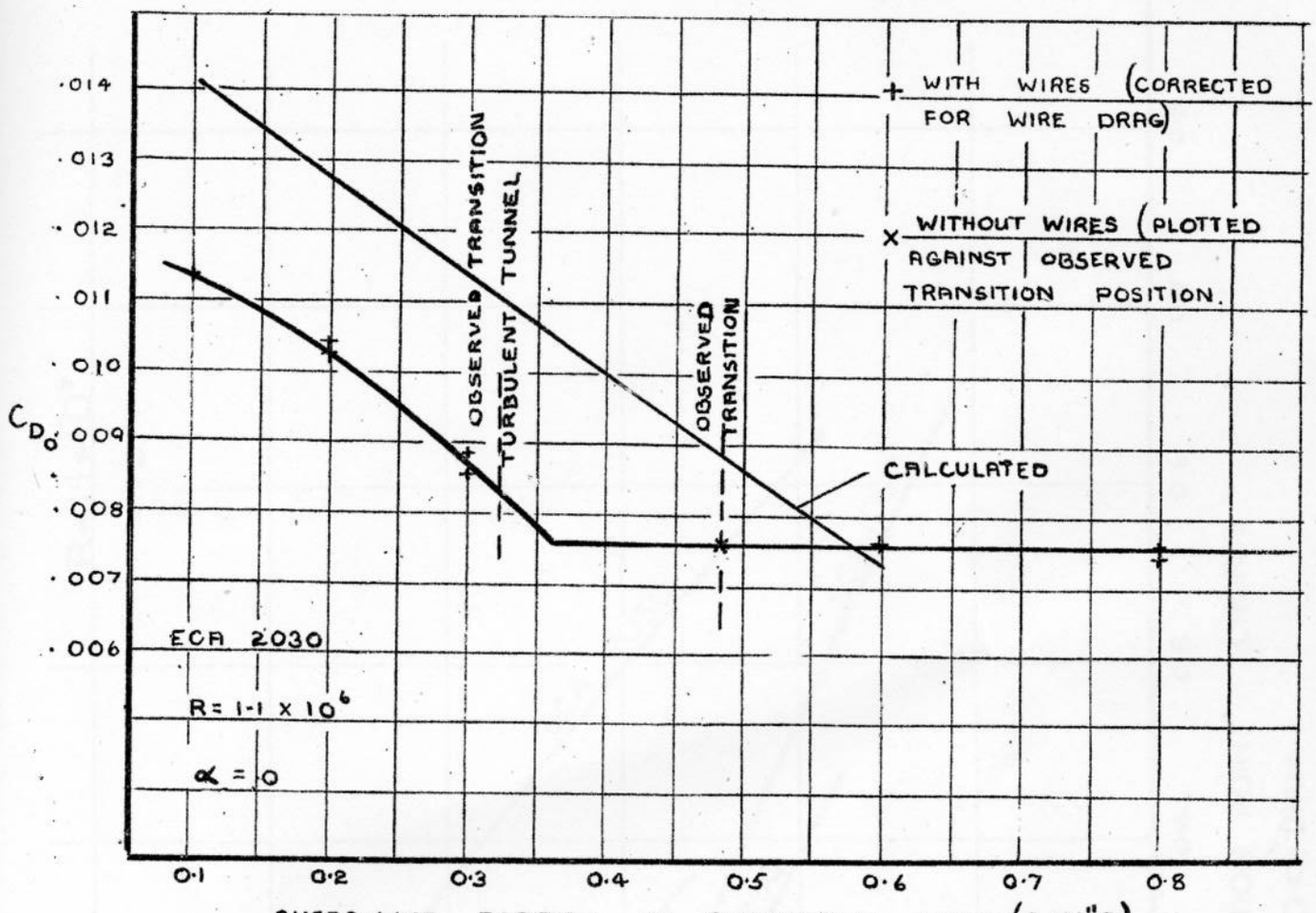

FIG 17

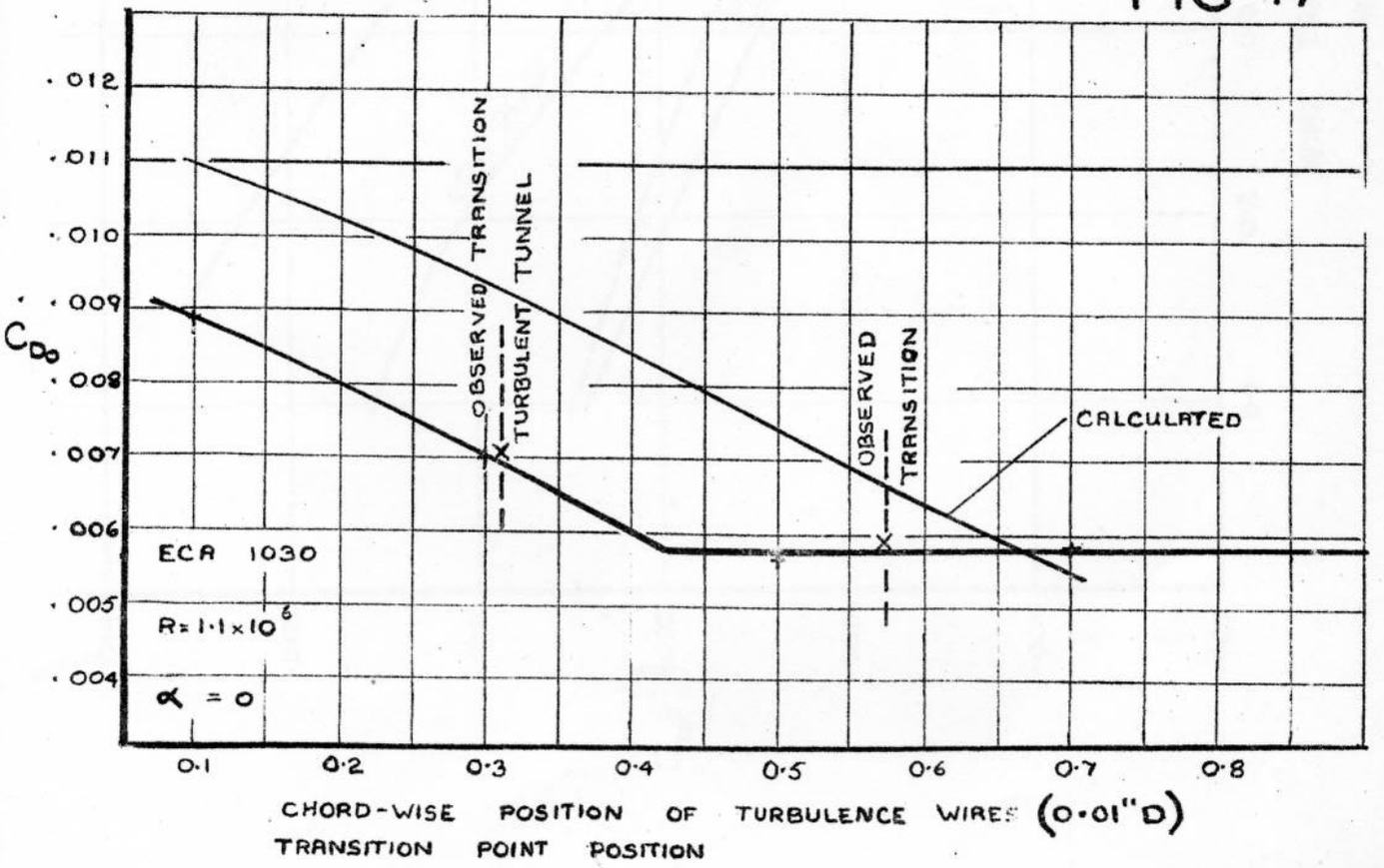

FIG 18

VARIATION OF DRAG COEFFICENT "WITH WIRE TRANSITION POINT" FOR ECA AEROFOILS EXPERIMENTAL

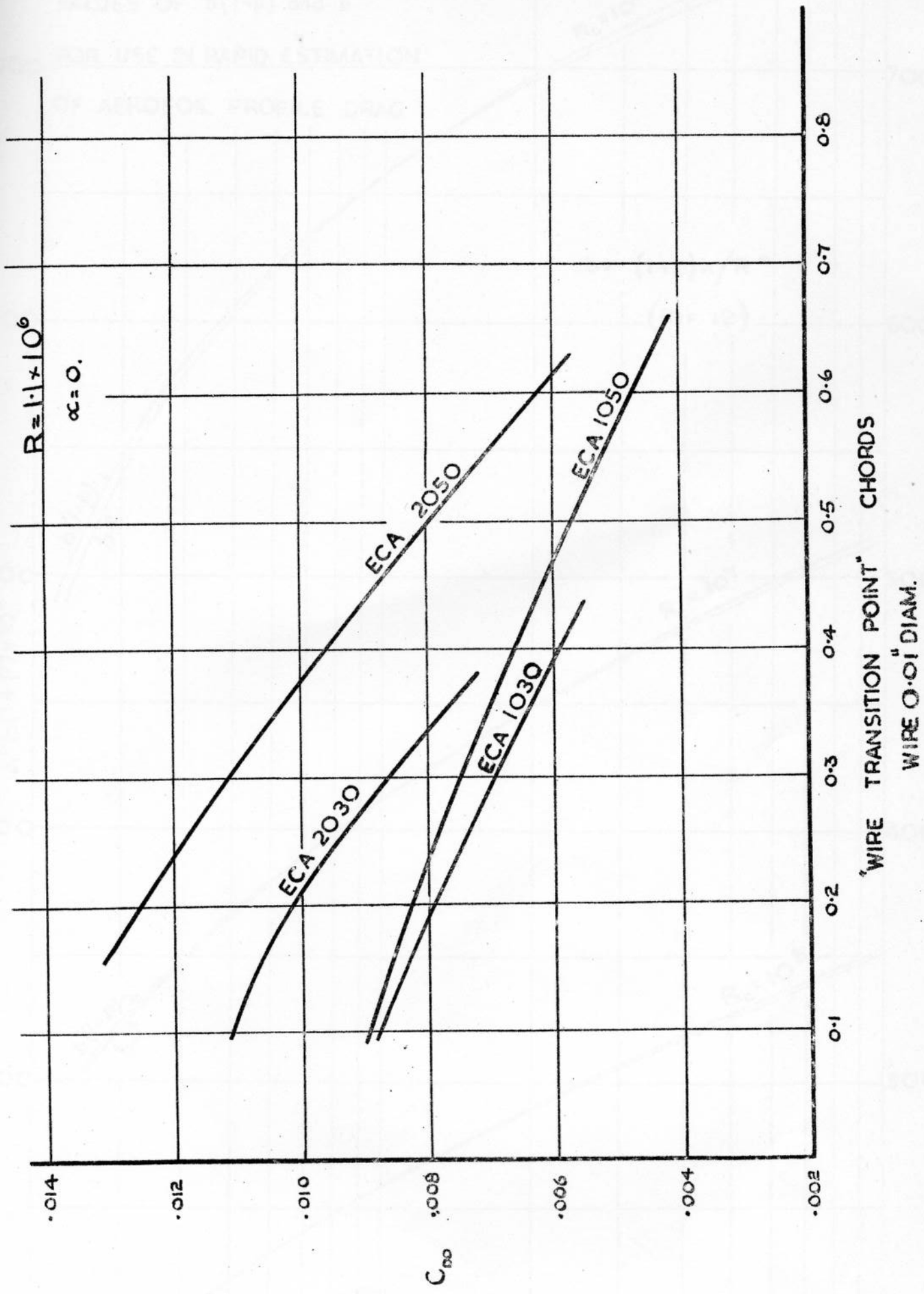

FIG 19

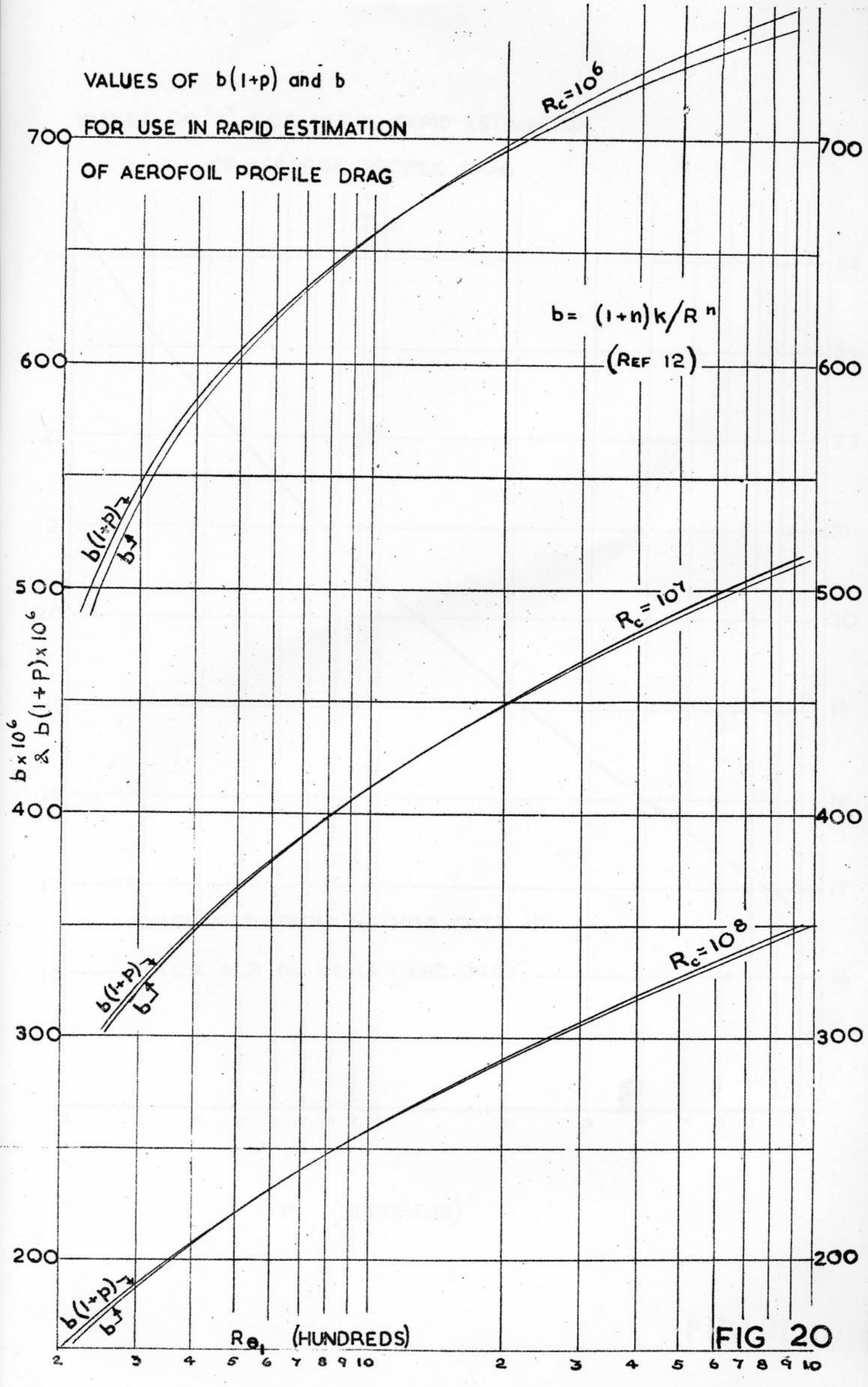
VALUES OF b(1+p) and b
FOR USE IN RAPID ESTIMATION
OF AEROFOIL PROFILE DRAG
b= (1+n)k/R^n
(REF 12)
Rc=10^6
Rc=10^7
Rc=10^8
b(1+p)→
b→
b×10^6 & b(1+p)×10^6
700
600
500
400
300
200
Re1 (HUNDREDS)
2 3 4 5 6 7 8 9 10 2 3 4 5 6 7 8 9 10

FIG 20

VALUES OF "n" FOR USE IN RAPID ESTIMATION

OF AEROFOIL PROFILE DRAG

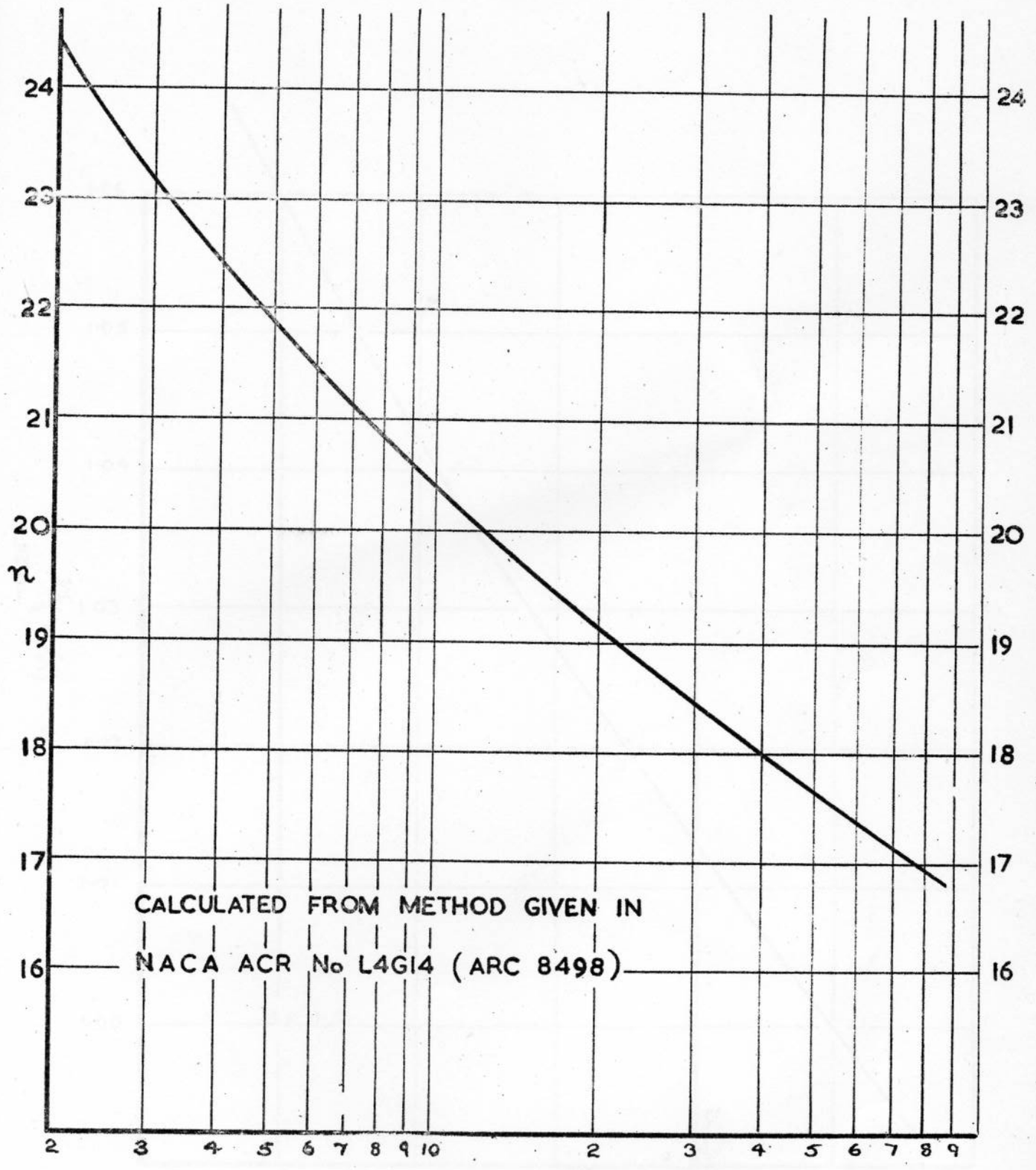

FIG 21

VALUES OF "a" FOR USE IN RAPID ESTIMATION OF AEROFOIL PROFILE DRAG

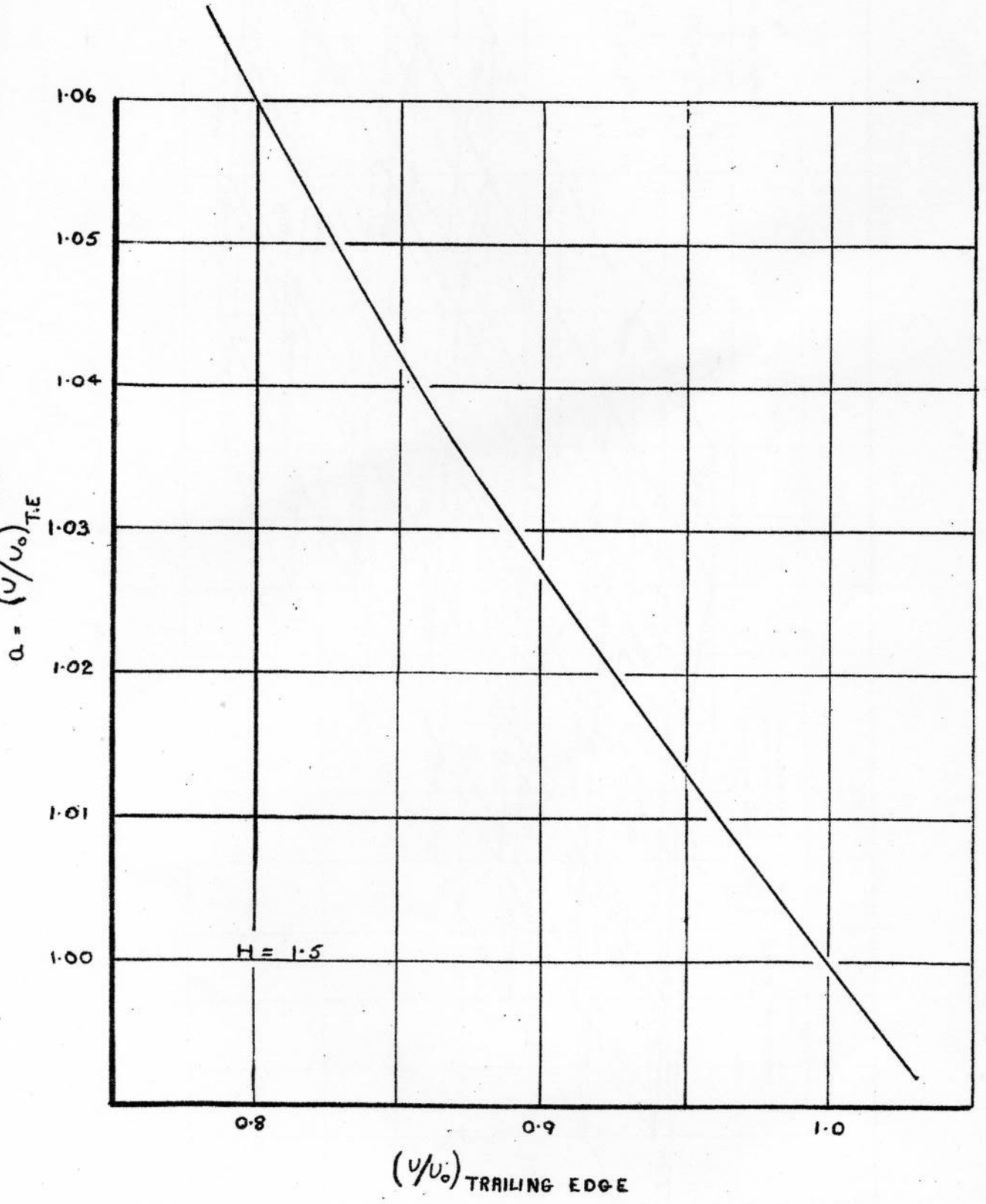

FIG 22

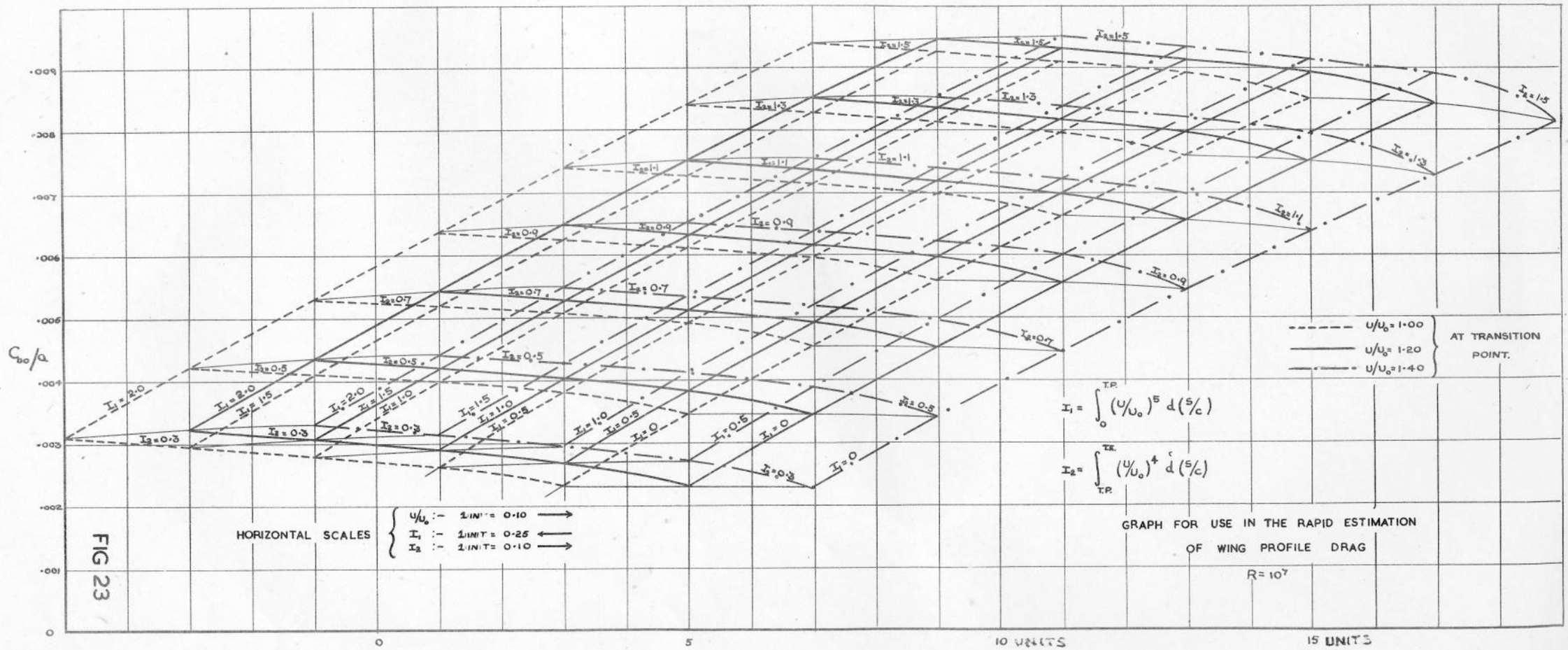
C_{bo}/a
·009
·008
·007
·006
·005
·004
·003
·002
·001
0
0
5
10 UNITS
15 UNITS
$I_1 = 2·0$
$I_1 = 1·5$
$I_1 = 1·0$
$I_1 = 0·5$
$I_1 = 0$
$I_2 = 1·5$
$I_2 = 1·3$
$I_2 = 1·1$
$I_2 = 0·9$
$I_2 = 0·7$
$I_2 = 0·5$
$I_2 = 0·3$
HORIZONTAL SCALES
U/U_o :- 1 INIT = 0·10
I_1 :- 1 INIT = 0·25
I_2 :- 1 INIT = 0·10
$U/U_o = 1·00$
$U/U_o = 1·20$
$U/U_o = 1·40$
AT TRANSITION POINT.
$I_1 = \int_{T.P.}^{0} (U/U_o)^5 \, d(s/c)$
$I_2 = \int_{T.P.}^{0} (U/U_o)^4 \, d(s/c)$
GRAPH FOR USE IN THE RAPID ESTIMATION OF WING PROFILE DRAG
$R = 10^7$

FIG 23